Renewable and Sustainable Energy Reviews 22 (2013) 148–167

Contents lists available at SciVerse ScienceDirect

Renewable and Sustainable Energy Reviews

journal homepage: www.elsevier.com/locate/rser

Quantum dot-sensitized solar cells—perspective and recent developments: A review of Cd chalcogenide quantum dots as sensitizers

H.K. Jun, M.A. Careem, A.K. Arof*

Centre for Ionics, Department of Physics, Faculty of Science, University of Malaya, 50603 Kuala Lumpur, Malaysia

ARTICLE INFO

Article history:
Received 30 April 2012
Received in revised form
7 January 2013
Accepted 14 January 2013
Available online 1 March 2013

Keywords:
Quantum dot-sensitized solar cells
Cadmium chalcogenide
Power conversion efficiency
Quantum dots

ABSTRACT

The emergence of quantum dot-sensitized solar cells (QDSSCs) has provided an alternative way to harvest sunlight for energy conversion. Among all the QDSSCs, cadmium chalcogenide (CdX, X=S, Se or Te) based QDSSCs have gained a significant interest due to their easy fabrication, low cost and high performance. However, their performance still does not match with that of their dye-sensitized solar cells (DSSCs) counterpart. In this review, the concept and mechanism behind the QDSSCs are reviewed. Fabrication methods and possible approaches for improving the Cd chalcogenide QDSSC performance are also discussed. It is worthwhile to note that the efficiency of a QDSSC depends on the fabrication method of the quantum dots, morphology of the photoanode, type of electrolyte used and the choice of the counter electrode. It is therefore, imperative for engineering of materials and optimization of the fabrication method for the improvement of QDSSCs performance.

Contents

* Corresponding author. Tel.: +60 3 7967 4085.
E-mail address: akarof@um.edu.my (A.K. Arof).

1364-0321/$ - see front matter © 2013 Elsevier Ltd. All rights reserved.
http://dx.doi.org/10.1016/j.rser.2013.01.030

1. Introduction

Renewable energy has been a global issue in recent years. Due to limited fossil fuel reserve and global warming issues, demand for renewable energy has increased. Solar energy has emerged as a potential and marketable alternative energy. Energy from sunlight that reaches the Earth in one hour (4.3×10^{20} J) alone is sufficient to fulfill the energy consumption on the planet in a year (4.1×10^{20} J) [1]. The tapping of sunlight energy has been made easy with the introduction of low-cost and high-efficiency solar cells. A wide range of solar cell technologies are being researched and developed currently, which includes dye-sensitized nanocrystalline solar cells [2], bulk heterojunction solar cells [3,4], depleted heterojunction solar cells [5,6], and hybrid organic–inorganic solar cells [7–9].

Chronologically, solar cell technologies have evolved into three generations [10]. First generation photovoltaic cells are based on a single crystalline semiconductor wafer. Second generation photovoltaic solar cells utilize inorganic thin film structure in the cell assembly. They are cheaper to produce, but the efficiency, which is less than 14% in amorphous thin film solar cells is lower than the efficiency exhibited by the single junction crystalline photovoltaic cell of the first generation that can reach as high as 27%. Theoretically, single junction cells should be able to exhibit a maximum efficiency of ~33% [11], a limit set by Shockley–Queisser thermodynamics. Thus, a new solar cell technology is required in order to achieve efficiencies greater than 33% with lower production cost. The onset of this breakthrough is the third generation photovoltaic cells [12]. The relation between the photovoltaic production cost per square meter with the solar cell module efficiency and the cost per unit power are shown in Fig. 1 [13]. It is predicted with the emergence and advancement of the third generation photovoltaic cells, higher efficiency devices are possible with lower production cost. Some examples of solar cells which fall under this category are dye-sensitized solar cells (DSSCs), quantum dot-sensitized solar cells (QDSSCs), colloidal quantum dot solar cells (CQD), organic solar cells, etc.

Low-cost and high-efficiency solar cells were first introduced as DSSCs with inorganic ruthenium based dyes in early 90s [14]. From then onwards, numerous researches have been focused on the development and characterization of different dyes for application in DSSCs. These include but not limited to natural dye materials [15,16] and synthetic organic dyes [17]. Based on the DSSC's structure, quantum dot (QD) was introduced as a

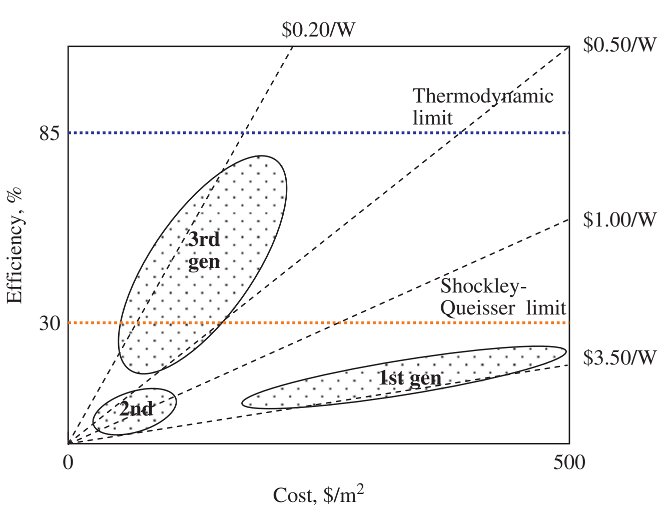


Fig. 1. Efficiency-cost trade-off for the three generations of solar cell technology, wafers, thin-films and advanced thin-films (year 2003 dollars). Adapted from Ref. [13].

replacement of dye due to its excellent opto-electronic properties [2,18,19]. QDs are nano-sized semiconductor particles whose physical and chemical properties are size-dependent. Among the notable characteristics of QDs include tunability of band gap energy, narrow emission spectrum, good photostability, broad excitation spectra, high extinction coefficient and multiple exciton generation [20–23]. With these advantages, researchers were able to fabricate solar cell devices achieving efficiency up to 7% in QD related solar cells [24,25]. Other upcoming trend is "green" QDSSC where less hazardous precursors are used during the preparation of QDs [26].

Over the last few years, cadmium chalcogenide (CdX, X=S, Se or Te) QDs have attracted more attention in QDSSC research. The widespread of research activities in CdX QDs are due to their distinct properties such as ease of fabrication, tunability of band gap energy through size control and possible multiple exciton generation as mentioned above. It is noted that CdX absorbs photon efficiently because it has a bulk material band gap above 1.3 eV (band gap for CdS, CdSe and CdTe are 2.25 eV, 1.73 eV and 1.49 eV respectively) [27]. By altering the QD size, the band gap can be tuned further to match a desired band gap range. It is therefore critical to understand the physics and chemistry of these CdX QDs for a better research focus.

This short review will concentrate on the concepts of the QDSSC with emphasis on cadmium chalcogenide (CdX, X=S, Se or Te) as QD sensitizers. The fundamental electrical characteristics of solar cells will be first reviewed. This will be followed by basic working principles of the QDSSC. Subsequent sections are dedicated to the synthesis methods and sensitization with CdX QDs. Finally, the methods used to improve the performance and the stability of the CdX QDSSCs will be discussed.

2. Basic principles of QDSSCs

2.1. Structure of a DSSC and QDSSC

A typical DSSC consists of a dye-sensitized photoanode (working electrode) and a counter electrode (CE) separated by a salt electrolyte [28]. Photoanode consists of a mesoporous wide band gap semiconductor layer that is attached to the conducting glass. Typically, TiO_2 is chosen for the mesoporous semiconductor although other oxides such as ZnO and Nb_2O_5 are possible [19,29,30]. A monolayer of charge transfer dye is then attached on the surface of the mesoporous wide band gap semiconductor. This photoanode section is in contact with a redox electrolyte or hole conductor. The structure is completed by coupling with a counter electrode (cathode) as shown in Fig. 2.

The evolution of DSSC to QDSSC does not take a big leap. The only physical difference between the DSSC and QDSSC is the sensitizing materials. In the QDSSC, the dye is replaced by inorganic nanoparticles of QDs [31]. The mesoporous TiO_2 is coated with these QDs using colloidal QD or in situ fabrication [18,32–34]. A general structure of a QDSSC and its operation is depicted in Fig. 3.

2.2. Performance parameters

The function of a conventional photovoltaic solar cell is based on the formation of an electrical barrier between n- and p-type semiconductors. The potential difference across this barrier creates an electrical diode structure. Thus, the current–voltage characteristic of the solar cell follows the diode equations. Fig. 4 is an illustration of current–voltage characteristics of a solar cell in the dark and under illumination conditions.

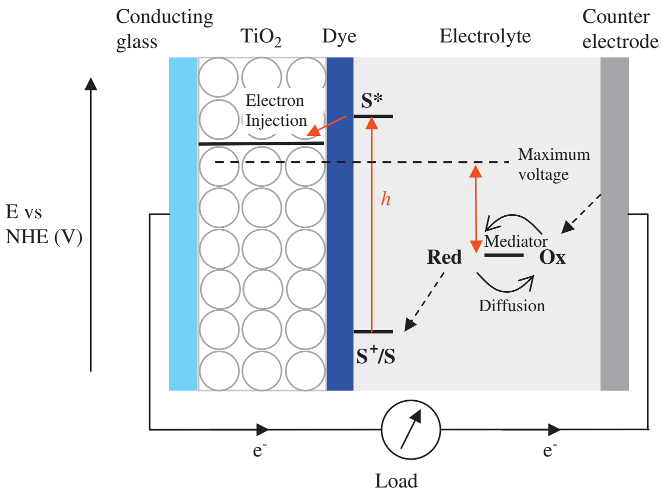


Fig. 2. Structure and operating principle of a typical DSSC.

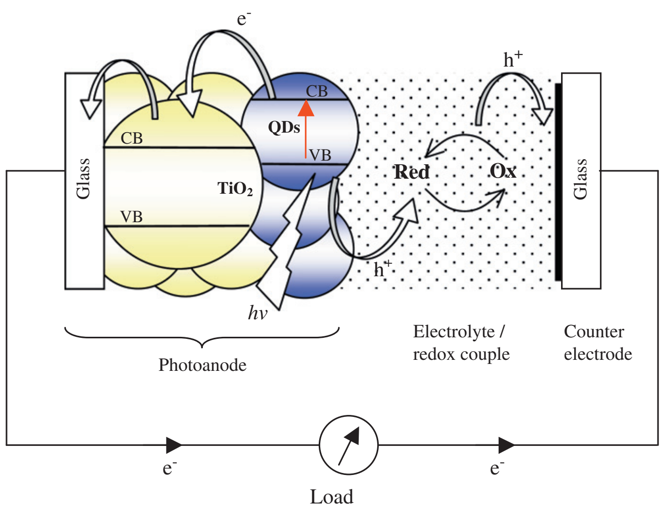


Fig. 3. Structure and operating principle of a typical QDSSC.

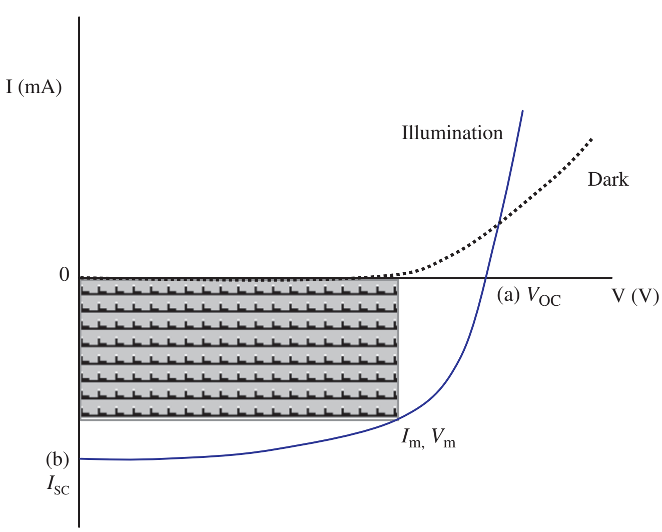


Fig. 4. Current–voltage curves of a photovoltaic solar cell under dark and illuminated conditions. The intersection value with the abscissa and ordinate are the open-circuit voltage (V_{oc}) and the short-circuit current (I_{sc}) respectively. Maximum power output, P_{max}, is determined by the maximized product of I_m and V_m. By dividing the P_{max} with the product of I_{sc} and V_{oc}, it results the fill factor (FF).

Under the dark condition, there is no current flowing. However, when sufficiently high voltage is applied i.e. higher than open circuit voltage, the contacts start to inject carriers to produce current at forward bias. Upon light illumination, additional photocurrent will be generated and flow across the junction. The maximum generated photocurrent contributes to the short-circuit current (I_{sc}) at (b). During open circuit when there's no current flowing, the open-circuit voltage (V_{oc}) is defined at (a). Power output then can be determined from the product of current and voltage in the fourth quadrant of the current–voltage curve. At the maximum power point (I_m and V_m), the product is the largest, where the maximum rectangle area in the figure meets the curve [7]. This defines the fill factor (FF).

$$FF = (I_m \times V_m)/(I_{sc} \times V_{oc}) \quad (1)$$

The maximum theoretical FF value is 1.0. However, in reality the value is limited to 0.83 based on the diode Eq. [1]. The photovoltaic power conversion efficiency,η, is defined by the electrical power density divided by the incident solar power density (P). P is standardized at 1000 W m^{-2} for photovoltaic cell tested at spectral intensity matching the sun's intensity on earth's surface at an angle of 48.2° (equivalent to AM 1.5 spectrum) [7].

$$\eta = I_m \times V_m/P \quad (2a)$$

$$\eta = I_{sc} \times V_{oc} \times FF/P \quad (2b)$$

QDSSCs also function like junction solar cells under dark and illuminated conditions and therefore, their performance parameters can also be obtained using the above equations.

In a three-electrode measurement, conversion efficiency is measured as incident photon to current efficiency (IPCE). IPCE is a measure of ratio of charge carriers collected at the electrodes to the number of incident photons, also known as external quantum efficiency. IPCE at different wavelengths is determined from the short circuit photocurrents (I_{sc}) observed at different excitation wavelengths using the expression [7]

$$IPCE\ \% = (1240 \times I_{sc})/(\lambda \times I_{inc})100 \quad (3)$$

where I_{inc} is the incident light power (*i.e.* the energy of the light incident on the electrode) and λ is wavelength. For an ideal solar cell, the I_{sc} value can be determined from the IPCE data with the standard AM 1.5 spectrum. However, in QDSSC, the case is not ideal. Thus the calculated I_{sc} might be an approximation for the measured I_{sc} under 1 sun (1000 W m^{-2}) [21].

2.3. Working mechanism

The working mechanism of the QDSSC is very similar to that of the DSSC. When the QDs (CdX, X=S, Se or Te) are subjected to band gap excitation, upon illumination, electron–hole pairs are formed in the QDs. The electrons will enter into the conduction band (CB) of the QD and the hole remains in the valence band (VB). The excited QD injects the electron from its CB into the CB of the wide band gap semiconductor (e.g. TiO_2) and in doing so it itself is oxidized with the hole remaining in the valence band. The injected electron from the QD percolates through the porous TiO_2 network and ultimately reaches the conducting glass. From there it travels through the external load and completes the circuit by entering back through the counter electrode. The generated voltage is perceived as an evidence of the solar energy conversion to electric energy. This voltage corresponds to the difference between the quasi-Fermi level of the electron in the photoanode and the redox potential of the polysulfide electrolyte [30], which usually consists of a (S^{2-}/S_x^{2-}) redox couple. The oxidized QD is then restored (hole is filled with electron) when it is reduced by S^{2-} from the electrolyte and in turn it is oxidized

into S_x^{2-} that diffuses to the counter electrode. Chemically, the following reactions take place where oxidation occurs at the photoanode–electrolyte interface [35]

$$S^{2-}+2h^{+}\rightarrow S \quad (4)$$

$$S+S_{x-1}{}^{2-}\rightarrow S_x{}^{2-}(x=2-5) \quad (5)$$

and at the counter electrode, reduction occurs where the S_x^{2-} is reverted back to S^{2-}

$$S_x^{2-}+2e^{-}\rightarrow S_{x-1}^{2-}+S^{2-} \quad (6)$$

The whole key processes of the photocurrent generation can be illustrated as in Fig. 5. It should be concluded that QDs have a photovoltaic response upon illumination which results in photocurrent and voltage generation. They have the tendency of charging up to a state that changes the relative energetics within the cell which ultimately influence the generation and recombination processes [36].

3. Transport processes and properties of QDSSCs

3.1. Charge separation and transport

In the DSSC, charge separation occurs at the interface between wide band gap semiconductor/dye and electrolyte. For QDSSC, charge separation reactions are at the surface between wide band gap semiconductor/QD and redox electrolyte. Upon illumination, the excited QDs will generate electron–hole pairs [37–39]

$$CdX+h\nu\rightarrow CdX(e+h) \quad (7)$$

where e and h denote electron and hole generated, respectively. At the interface between TiO_2 and the excited QDs, charge transfer takes place

$$CdX(e+h)+TiO_2\rightarrow CdX(h)+TiO_2(e) \quad (8)$$

$$CdX(h)+Red\rightarrow CdX+Ox \quad (9)$$

where Red and Ox are the reduced and oxidized conditions of the electrolyte. Thus, for CdX–TiO_2 system with polysulfide redox couple, the following reaction can be expressed as

$$CdX(h)+S^{2-}\rightarrow CdX+S\rightarrow CdX+S_x^{2-} \quad (9a)$$

It has been observed that the electron transfer is size-dependent especially in QD–TiO_2 system and that the charge injection dynamics are determined by the QDs [39]. Different pH electrolyte solution could also modulate the charge injection process when in contact with the photoanode as observed in fluorescence spectra reported by Chakrapani et al. [40]. At higher pH value (more alkaline), the CB of TiO_2 shifted to more negative potentials. This results in a decrease of the energy difference between CB band edges of QD and TiO_2. Consequently, electron injection rate would be decreased. One interesting point to take note is that there is no significant difference in the electron injection and recombination of injected electrons on the sizes of the QDs [41].

3.2. Advantages of QDs as sensitizers

Some of the advantages of QDs are tunable energy gaps, ability of multiple exciton generation, photostability, low cost and high absorption coefficient, which is known to reduce the dark current and increase the overall efficiency of solar cells [42]. Of all these, tunable energy gaps and multiple exciton generation features are the most desirable characteristics of the QDs [20–23].

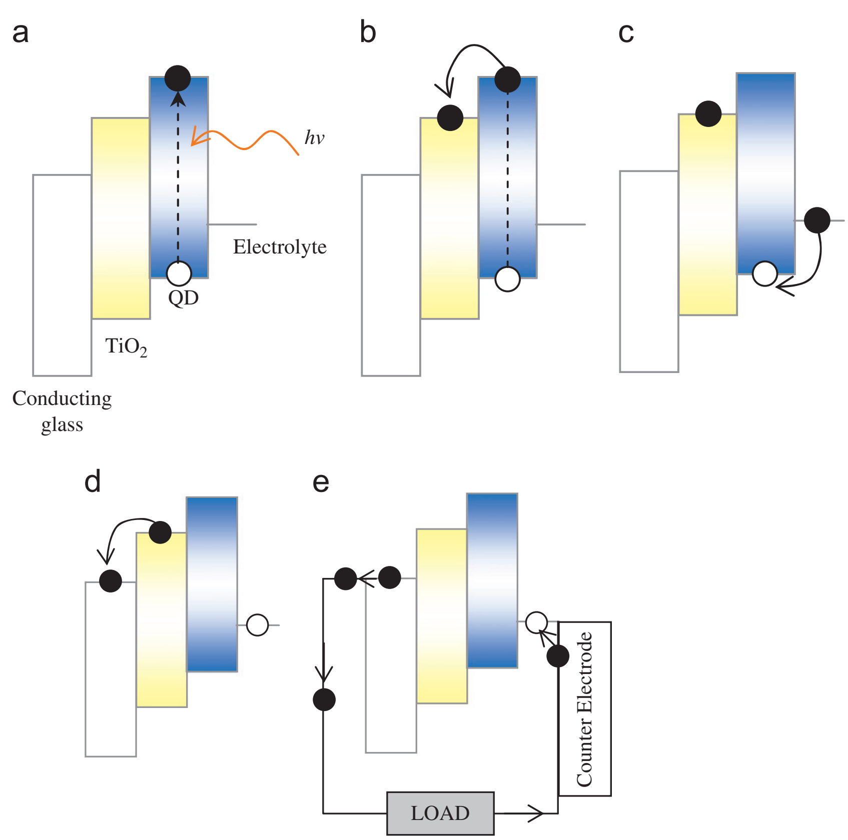


Fig. 5. Schematic of an energy diagram of a QDSSC stack under flat band conditions. Key processes leading to the generation of photocurrent are shown in (a)–(e).

3.2.1. Tunable energy gaps

Various research groups have studied the ability of QDs as sensitizers in QDSSCs [22,23,31,43]. The QD properties mentioned in the preceding sections are not only limited to Cd chalcogenides but applicable to other QD materials as well. The main motivation of using QDs as sensitizers in solar cell is due to their tunable energy band gaps, which can control their absorption range [19]. There are several reports in the literature showing that CdS and CdSe with tunable band gaps property are capable of converting visible light to electric energy [39,44]. Vogel et al. [19] demonstrated that efficient charge separation can be optimized by tuning the size of the QDs utilizing the quantization effect. Kongkanand et al. [39] separately reported that by varying the size of CdSe QDs assembled on TiO_2 films, improvement in photoelectrochemical response and photoconversion efficiency can be obtained (Fig. 6). With the decrease of CdSe particle size, photocurrent increases due to the shift of the CB to more negative potentials which in turn increases the driving force for charge injection. As a result, higher IPCE is obtained at the excitonic band. On the other hand, if the particle size is increased, the particles will have better absorption in the visible region. The disadvantage of this is lower effectiveness of electron injection into TiO_2 as compared with smaller-sized CdSe QDs.

This size dependent effect is made possible due to the quantum confinement effect exhibited by the QD itself [43,45]. Quantum confinement effect can be manifested when QDs in colloidal solution show different color corresponding to the change of particle size, which influences a different absorption band of light. When the QD particles are sufficiently small, the effective band gap energy of the QD is wider. Subsequently, the optical absorptions and emissions in relation with excitations across the band gap shift towards higher energies [21]. Quantum size effects have been demonstrated by Gorer et al. with the observed blue shift of the optical spectra of CdSe films as the crystal size decreases [46]. This phenomenon is also highlighted in CdS QDs, as reported by Thambidurai et al. [47] where the same blue shift was observed in the optical spectra of smaller CdS QDs. Therefore, we can conclude that a combination of different quantum dot sizes in a cell will have better efficiency due to wider absorption of light by the quantum dots having a range of band gaps.

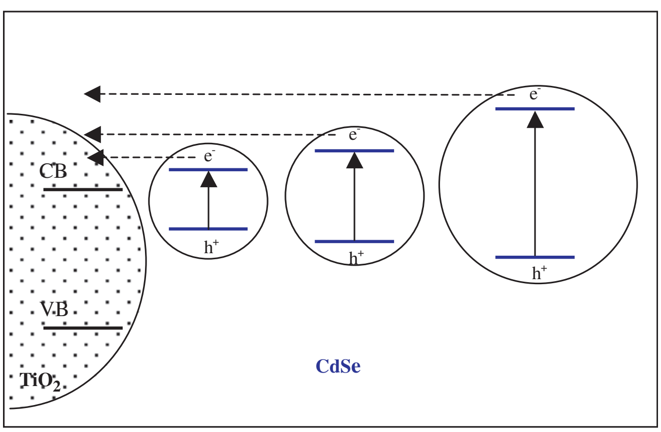


Fig. 6. Schematic diagram illustrating the energy levels of different-sized CdSe QDs and TiO2. (The injection of electrons from CdSe QDs into TiO_2 is influenced by the energy difference between the two conduction bands. Note that band positions are for reference only and not to scale). Adapted from Ref. [39].

3.2.2. Multiple exciton generation

Multiple exciton generation (MEG) in QDs from a single photon have been widely studied [31,48–54]. In general, it is the generation of more than one electron–hole pair upon the absorption of a photon. This phenomenon was first demonstrated in PbS and PbSe QDs systems in year 2004–2005 [48–50]. However, subsequent studies revealed that multiple exciton generation has not been detected in CdSe and CdTe QDs systems [55] though some latest investigations showed positive results [53,56,57]. The process could be mediated by different mechanisms in CdSe nanoparticles. Essentially, multiple excitons are generated when hot carriers produce more than one electron–hole pair through impact ionization. More details of MEG can be found in the review by Nozik [31].

Upon absorption of solar radiation, photon with energies greater than the band gap creates electrons and holes. At this point, the excess kinetic energy is equal to the difference between the photon energy and the band gap, which creates an effective temperature condition for the carriers. The temperature of the carriers is higher than the lattice temperature. Thus, the term hot carriers (or hot electrons and hot holes) is used.

The inverse of impact ionization is the Auger process, which is the recombination of two or more electron/hole pairs to produce a single energetic electron–hole pair. Given the possibility of Auger process, it is imminent that the impact ionization process to be faster than the carrier's cooling or relaxation rate. To remedy this, the hole is usually removed from the QD's core by a fast hole trap at the surface which eventually block the Auger process [31]. A simple schematic diagram depicting the impact ionization and Auger recombination is shown in Fig. 7. Efficient multiple exciton generation is predicted to enhance the conversion efficiencies of QDSSC up to 44% [58].

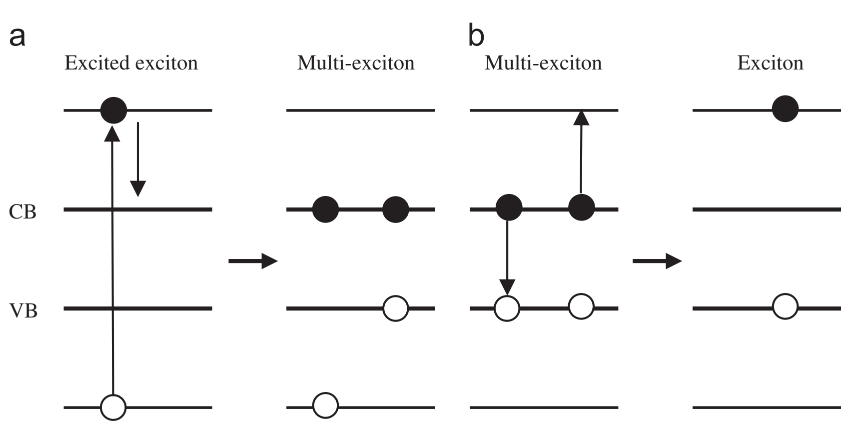


Fig. 7. Schematic diagram of (a) impact ionization and (b) Auger recombination processes. Electrons (filled circles), holes (empty circles), conduction band (CB) and valence band (VB).

4. Preparation of quantum dot sensitizers

There are various methods for preparing QDs and attaching them to the wide band gap semiconductor material [59]. Generally, these methods can be categorized into two major methods: in situ fabrication and attachment of pre-synthesized colloidal QD. In situ fabrication method is the most used approach for QDs preparation. It is facile and low cost. Chemical bath deposition (CBD) and successive ionic layer adsorption and reaction (SILAR) are two well known in situ techniques. Not only the techniques are simple, but they also can be used in large scale production. However, these techniques do not allow precise control of the particle size distribution of the QDs.

The other approach is to use pre-synthesized QDs (also known as ex situ fabrication). QDs are usually prepared ex situ and adsorbed on wide band gap semiconductor surface by using molecular linkers that have various functional groups. QDs can also be deposited directly without using linker molecules. This technique enables the precise control over the size and hence the spectral absorption properties of the QDs.

4.1. Chemical bath deposition (CBD)

In the CBD method, nucleation and growth of QDs take place in one bath. Cationic and anionic solutions are prepared separately and placed in a container to form a bath solution for slow reaction. QDs are grown on the surface of the wide band gap semiconductor on an electrode surface by dipping the electrode into the bath solution for a defined period. Thus, the QDs deposition is controlled by varying the dipping time. This method has been used to attach CdS and CdSe QDs onto wide band gap semiconductors [33]. Recently, a new type of CBD approach has been introduced which is referred to as sequential CBD (S-CBD) [60]. This method is however, very similar to the SILAR method described below. In a latest development, microwave assisted CBD is used and this method is capable of producing QDs that can improve the short circuit current density as well as power conversion efficiency in QDSSCs [61,62]. Here the deposition of QDs is done with TiO_2 electrode immersed into a sealed container containing a precursor aqueous solution. The container is then put into a microwave system for a suitable microwave treatment. The addition of the microwave step can spur faster nucleation and growth of QDs. Zhu et al. [61,62] claim that this procedure enable fast deposition of CdS layer which assists in suppressing carrier recombination at the surface defects of QDs as well as facilitate easy attachment of QDs. Table 1 gives the summary of other groups who have used CBD technique to prepare the QD-sensitized photoanodes.

4.2. Successive ionic layer adsorption and reaction (SILAR)

The SILAR method is an extension of CBD technique. In this approach, cationic and anionic precursors are separately placed in two beakers or containers. TiO_2-coated electrode is dipped into the cationic precursor solution followed by rinsing and drying. Then it is dipped into the anionic precursor solution and completed with a final rinsing and drying. The two-step dipping is regarded as one deposition or SILAR cycle. The size of the deposited QDs can be controlled by the number of dip cycles. Within a cycle, each dipping period can be tailored to achieve the desired particle size growth. This method is designed such that the particle size will increase by one monolayer during a dip or immersion cycle. SILAR is a better approach when compared with CBD because of its shorter processing time and close stoichiometry formation as reported by Senthamilselvi et al. [63]. This method has been successfully utilized to synthesize CdS, CdSe and CdTe onto TiO_2 film [64,65]. In a recent work by Barcelo et al. [66], SILAR has been shown to be advantageous when applied to ZnO mesoporous electrode due to its simplicity, homogenous QD distribution, high QD coverage degree and high IPCE values obtained in QDSSCs. The reader is referred to Table 1 for finding other research groups who have used the SILAR method to prepare QDs.

4.3. Surface attachment through molecular linkers for ex situ fabrication of QDs

For QD deposition via surface attachment, QDs are first pre-synthesized using capping agents. Capping agents are responsible in controlling the nanostructure shape, size and optical properties. Some examples of capping agent are mercaptopropionic acid (MPA), trioctylphosphine (TOP) and trioctylphosphine oxide (TOPO). Synthesis is performed in a vessel where the metal precursor (e.g. CdO) is heated before the inclusion of the next organometallic precursor (e.g. TOP-Se solution). Removing the heat will stop the growth reaction. In other words, QD size is controlled via temperature and also the capping agent concentration. One needs to monitor the growth by UV/Vis spectroscopy. Thus, a series of experiments should be performed to determine the size of QDs formed at a specific temperature and concentration of the capping agent. After the QDs are synthesized, the wide band gap semiconductor coated electrode is immersed in a solution containing bifunctional molecular linkers (in this case is the capping agent such as MPA). The immersion causes the functional group of the linker to attach onto the semiconductor surface while the other end of the functional group is available for QD attachment. Functional linking molecules assist in dispersing and stabilizing the QDs more effectively [67]. Subsequent immersion of the semiconductor electrode in a solution containing the QDs is needed to provide the adsorption of QDs onto the semiconductor film surface. The immersion may have to last from few hours to a few days, which is a very time consuming process as compared with the CBD or SILAR methods. During the QD solution immersion, ligand exchange takes place. Fig. 8 shows a schematic diagram of the process of molecular linking with QD and TiO_2 surface. Synthesis of CdX (X=S, Se, Te) using linker via wet chemical route has been first demonstrated by Murray et al. [68]. The other groups who have used this method for attaching QDs to the TiO_2 surface are listed in Table 1.

4.4. Other methods

Besides CBD, SILAR and linker assisted assembly, QDs can also be prepared and attached via direct adsorption (DA) or physisorption. In DA, QDs are attached on the wide band gap semiconductor film without the assistance of a molecular linker. DA may lead to a high degree of QD aggregation in addition to a low surface coverage [69,70]. However, QDs prepared by the DA method do give higher IPCE values in QDSSCs compared to those obtained with QDs prepared with molecular linker assisted adsorption as reported by Guijarro et al. [70]. In their work, an IPCE of 36% at the QD excitonic peak was observed.

A less explored technique has been reported in the review by Rühle et al. [21] is based on physisorption. Under this approach, bare semiconductor electrodes (e.g. TiO_2, ZnO) are dipped into solution of QDs up to 100 h. The literature on this approach is somewhat limited. However, photovoltaic cell performance of QDs attached via physisorption indicates a better result than the performance of cells with QDs prepared using molecular linker assisted adsorption.

In Wijayantha et al.'s [71] work, CdS QDSSCs were assembled via a pressing route where a polymer film was placed on the top of the

Table 1
Summary of QDSSCs with fill factors and power conversion efficiencies reported in recent literature.

No.	Author	Sensitizer	Wide band gap semiconductor	Electrolyte*	Counter electrode	QD deposition method	FF (%)	η (%)	Highlights	Ref.
1.	Vogel et al. (1990)	CdS	TiO_2	$KCl+Na_2S$	Pt	SILAR	–	–	Photocurrent efficiency above 70% and photovoltage of 400 mV.	[18]
2.	Liu and Kamat (1993)	CdSe	TiO_2	$[Fe(CN)_6]^{3-/4-}$	Pt	CBD	–	–	Improved photocurrent stability of CdSe film by coupling it with a TiO_2 particulate film.	[33]
3.	Fang et al. (1997)	CdSe, ZnTcPc	TiO_2	$Na_2S+Na_2SO_4$	Pt	CBD	–	–	First reported co-sensitization of TiO_2 electrode by combination of CdSe particles and phthalocyanine.	[187]
4.	Peter et al. (2002)	CdS	TiO_2	Na_2SO_3	Pt	Linker	–	–	Sensitization of mesoporous TiO_2 with CdS QDs with controllable absorption edge.	[188]
5.	Toyoda et al. (2003)	CdS	TiO_2	$KCl+Na_2S$	Pt	SILAR	–	–	Increased photoelectrochemical current intensity with multiple CdS coating layer.	[64]
6.	Shen et al. (2004)	CdSe	TiO_2	$KCl+Na_2S$	Pt	CBD	–	–	Dependency of photoelectrochemical currents of the photoanode on the microstructure and electron diffusion coefficient in the electrode.	[189]
7.	Toyoda et al. (2005)	CdSe	TiO_2	$KCl+Na_2S$	Pt	CBD	–	–	Rutile-type content is advantageous to the photoelectrochemical properties of TiO_2 electrodes.	[190]
8	Nitsoo et al. (2006)	CdS, CdSe	TiO_2	$Na_2S+S+NaOH$	Pt	CBD	39.5	2.8	Improved cell parameters by selenization of the Cd-rich CdS layer with selenosulphate solution.	[191]
9.	Robel et al. (2006)	CdSe	TiO_2	Na_2S	Pt	Linker	–	–	12% IPCE with TiO_2–CdSe composite as a photoanode.	[37]
10.	Shen et al. (2006)	CdSe	TiO_2	$KCl+Na_2S$	Pt	CBD	–	–	45% IPCE in CdSe-sensitized TiO_2 nanotubes and nanowires with increased electrode thickness.	[192]
11.	Chang and Lee (2007)	CdS	TiO_2	$LiI+I_2$+DMPII+TBP in MPN	Pt	CBD	63	1.84	Well-covered CdS on the surface of TiO_2 mesopores via CdS-sensitized TiO_2 using modified CBD in alcohol.	[193]
12.	Diguna et al. (2007)	CdSe	TiO_2	Na_2S+S	Pt	CBD	50	2.7	Improved performance of CdSe-sensitized TiO_2 inverse opal by surface modification with ZnS layer and fluoride ions.	[122]
13.	Lee et al. (2007)	CdSe, CdTe	TiO_2	$LiI+I_2$ in ACN	Pt	Linker	67	<0.1	First reported quantitative cell tests using colloidal CdSe and CdTe QDs.	[84]
14.	Leschkies et al. (2007)	CdSe	ZnO	I_2+4TBP+LiI	Pt	Linker	30	0.40	Internal quantum efficiencies of 50-60% achieved with CdSe-sensitized ZnO nanowires.	[194]
15.	Lin et al. (2007)	CdS	TiO_2	$LiI+I_2$+DMPII+4TBP in MPN	Pt	Linker, CBD	60	1.35	Pre-assembled CdS QDs act as nucleation sites in the CBD process, forming nanofilm with an interfacial structure capable of inhibiting the recombination of injected electrons.	[195]
16.	Shen et al. (2007)	CdSe	SnO_2	$KCl+Na_2S$	Pt	CBD	–	–	Larger IPCE peak values ($\sim$20%) and integrated area for the IPCE spectra obtained with nanostructured SnO_2 electrodes.	[196]
17.	Kongkanand et al. (2008)	CdSe	TiO_2	Na_2S	Pt	Linker	40	0.70	Tubular morphology of CdSe-TiO_2 nanotube film in nanostructure-based solar cells.	[39]
18.	Lee et al. (2008)	CdSe	TiO_2	$[Co(o\text{-phen})_3]^{2+/3+}$ in ACN/EC	Pt	Linker	61	1.17	Stable performance of cells up to 42 days under room light condition using cobalt complex as a hole transporting material.	[164]
19.	Lee et al. (2008)	CdSe	TiO_2	Polysulfide	Pt	Linker	59	1.03	A co-sensitized TiO_2 electrode by CdSe and Mg-doped CdSe QDs displayed a broad spectral response in the 500-600 nm wavelength.	[197]
20.	Lee et al. (2008)	CdSe	TiO_2	Polysulfide	Pt	Linker	59	1.20	Co-sensitization of TiO_2 nanotubes with two different sizes of CdSe QDs showed higher performance than single size sensitization.	[198]
21.	Lee et al. (2008)	CdS	TiO_2	$Na_2S+S+KCl$ in methanol/H_2O	Pt	CBD	40	1.15	High IPCE of 80% obtained with polysulfide electrolyte in CdS-sensitized TiO_2 electrode.	[166]
22.	Lee et al. (2008)	CdS, CdSe	TiO_2	$Na_2S+S+KCl$ in methanol/H_2O	Pt	CBD	49	2.90	High efficiency in the CdSe-sensitized QD TiO_2 films coupled with CdS and ZnS coated layer.	[123]
23.	Lopez-Luke et al. (2008)	CdSe	TiO_2	Na_2S	Pt	Linker	27.7	0.84	Enhanced photoresponse in the near UV and visible region with CdSe QDs attached on nitrogen-doped TiO_2 nanoparticle.	[150]
24.	Mora-Sero et al. (2008)	CdSe	TiO_2	$Na_2S+S+NaOH$	Pt	Linker	43	0.40	IPCE value increased by 5–6 fold with the use of cysteine as functional linker between CdSe QDs and TiO_2.	[110]
25.	Shen et al. (2008)	CdS	TiO_2	$LiI+I_2$+DMPII+TBP in MPN	Pt	Linker	70	0.30	A well-covered QDs layer obtained from the adsorption of MSA-modified CdS QDs onto TiO_2 films using the carboxylic acid/TiO_2 interaction.	[42]
26.	Shen et al. (2008)	CdSe	TiO_2	Na_2S+S	Pt	CBD	31	2.02	Improved photovoltaic properties with ZnS modified CdSe-sensitized TiO_2 surface.	[124]

27.	Tachibana et al. (2008)	CdS	TiO_2	$[Fe(CN)_6]^{3-/4-}$	Pt	SILAR	60	1.00	Improved performance with a dense TiO_2 blocking layer on an FTO/TiO_2 mesoporous film.	[121]
28.	Bang and Kamat (2009)	CdSe, CdTe	TiO_2	Na_2S	Pt	Linker	–	–	Degradation of CdTe due to failure to scavenge photogenerated holes by a sulfide redox couple.	[167]
29.	Chen et al. (2009)	CdSe	ZnO	Polysulfide	Pt	Linker	34	0.45	Higher efficiency achieved with a layered structure of ZnO nanorods at the bottom and nanoflower on top than ZnO nanorods array alone.	[199]
30.	Chen et al. (2009)	CdSe	TiO_2	Na_2S+S	Pt	Linker	38.4	0.78	Lower efficiency but higher stability for QDSSCs with OA-capped CdSe photoanode.	[200]
31.	Chen et al. (2009)	CdSe	TiO_2	$LiI+I_2$+TBP+HMII in MAN	Pt	Linker	56.3	1.19	Improved performance of QDSSC due to higher loading and good coverage of QDs on TiO_2 film with optimal pH value at 7.	[111]
32.	Fan et al. (2009)	CdSe	TiO_2	Na_2S+S+KCl in methanol/H_2O	Pt	CBD	43	3.21	A highly efficient CdSe QDSSC prepared by a seed growing CBD process followed by addition of a ZnS film with post-sintering process to enforce the interface connection.	[201]
33.	Farrow and Kamat (2009)	CdSe	Carbon nanotube	Na_2S	Pt	Linker	–	<0.10	Increased photocurrent with addition of stacked-cup carbon nanotubes to the photoanode due to ultrafast electron transfer to the nanotubes.	[130]
34.	Gao et al. (2009)	CdTe	TiO_2	Na_2S	Pt	Linker	–	–	Improved photon response of CdTe-sensitized TiO_2 nanotubes compared to plain TiO_2 nanotubes film.	[202]
35.	Gimenez et al. (2009)	CdSe	TiO_2	Na_2S+S+NaOH	Cu_2S	DA	48	1.83	Improved efficiency of CdSe QDSSC prepared by DA with ZnS treatment and Cu_2S used as CE.	[69]
36.	Guijarro et al. (2009)	CdSe	TiO_2	N_2 purged Na_2SO_3	Pt	Linker, DA	–	–	A high degree of QD aggregation and IPCE value with CdSe-sensitized TiO_2 prepared by DA.	[70]
37.	Hossain et al. (2009)	CdS	TiO_2	Na_2S+S	Pt	CBD	26	1.13	Better photocurrent in CdSe-sensitized TiO_2 nanoparticles prepared by ammonia-free CBD with 12 min deposition time.	[203]
38.	Lan et al. (2009)	CdTe	TiO_2	$LiI+I_2$ in EMISCN	Pt	Linker	66	2.02	High efficiency obtained from the preparation of CdTe QDSSC with a simple heating process.	[204]
39.	Lee et al. (2009)	CdS, PbS	TiO_2	$[Co(o\text{-phen})_3]^{2+/3+}$ in ACN/EC	Pt	SILAR	–	1.13[a]	Cobalt complex as a redox couple was more efficient in generating photocurrents than Na_2S.	[165]
40.	Lee et al. (2009)	CdSe, CdTe	TiO_2	$[Co(o\text{-phen})_3]^{2+/3+}$ in ACN/ EC	Pt	SILAR	78	4.18	Overall conversion efficiency exceeding 4% obtained with CdTe-terminated CdSe QDSSC.	[65]
41.	Lee et al. (2009)	CdS	ZnO	$LiI+I_2$ in ACN	Pt	CBD	30	0.54	The morphology of the nanorods provides a direct pathway for the electrons from QDs to the photoanode.	[205]
42.	Lee and Lo (2009)	CdS, CdSe	TiO_2	Na_2S+S+KCl in methanol/H_2O	Au	CBD	49.0	4.22	High efficiency with cascade structure of CdS/CdSe QDs used as co-sensitizers where CdS was placed between CdSe and TiO_2.	[93]
43.	Sudhagar et al. (2009)	CdS:CdSe	TiO_2	Na_2S+S	Pt	CBD	42.3	2.69	Coupled CdS:CdSe QD-sensitized TiO_2 nanofibres provides a well-occupation of the pores by QDs and deeper electrolyte penetration.	[206]
44.	Sudhagar et al. (2009)	CdS	TiO_2	Polysulfide	Pt	CBD	49.6	1.28	Better interconnectivity among spheroidal particles and the mesoporous layer in CdS-sensitized TiO_2 nanospheroidal solar cells.	[207]
45.	Barea et al. (2010)	CdSe	TiO_2	Na_2S+S+NaOH	Pt	CBD	34	1.60	Increased photovoltaic performance by surface treatment of CdSe-sensitized TiO_2 with ZnS coating and molecular dipoles grafting.	[208]
46.	Chen et al. (2010)	CdS	TiO_2	$Na_2S+Na_2SO_3$	Pt	CBD	70	1.91	Improved efficiency by incorporating CdS QDs into TiO_2 nanorod array.	[132]
47.	Chen et al. (2010)	CdSe	Carbon nanotube+ZnO	Na_2S+S	Pt	Linker	57.5	1.46	An improved QDSSC based on vertically aligned carbon nanotube arrays coated with ZnO nanorods.	[140]
48.	Chen et al. (2010)	CdS, CdSe	ZnO	Na_2S+S	Pt	CBD	41.5	1.42	Broader light absorption range and better coverage of QDs on ZnO nanowires in CdS and CdSe co-sensitized ZnO nanowire.	[209]
49.	Chong et al. (2010)	CdSe	TiO_2	Na_2S+S+KCl	Au	SILAR	49	2.65	High efficiency of CdSe-sensitized TiO_2 by additional heat annealing which improved the interfacial and intra-connection among CdSe QDs.	[178]
50.	Deng et al. (2010)	CdS, CdSe	TiO_2	Na_2S+S	Cu_2S/C	CBD	58.1	3.08	Superior performance of QDSSC with nano-Cu_2S/C composite CE.	[182]
51.	Gonzalez-Pedro et al. (2010)	CdS, CdSe	TiO_2	Na_2S+S+NaOH	Cu_2S	SILAR	51	3.84	High efficiency of CdSe-sensitized TiO_2 with ZnS coating attributed to QDs in overcoming the photocurrent limit (or recombination).	[23]
52.	Guijarro et al. (2010)	CdSe	TiO_2	Na_2S+S+NaOH	Cu_2S	DA, Linker	58	1.49	Fast electron injection in CdSe-sensitized TiO_2 prepared by DA. DA process also yielded the slowest recombination.	[210]
53.	Huang et al. (2010)	CdS, CdSe	TiO_2	Na_2S+S	Cu_2S	CBD	58	3.18	Fibrous QDSSC prepared from CdSe-sensitized TiO_2 nanotubes on Ti wire with a ZnS passivation layer.	[211]
54.	Lee et al. (2010)	CdSe, Z907Na	TiO_2	$[Co(o\text{-phen})_3]^{2+/3+}$ in ACN/EC	Pt	SILAR	72	4.76	Effective redox couple based on cobalt complexes.	[106]
55.		CdS, CdSe	TiO_2		Pt	SILAR	49	3.90	Co-sensitization of CdS, CdSe and ZnS was able to increase the QDSSC performance.	[98]

Table 1 (*continued*)

No.	Author	Sensitizer	Wide band gap semiconductor	Electrolyte*	Counter electrode	QD deposition method	FF (%)	η (%)	Highlights	Ref.
	Lee et al. (2010)			$Na_2S+S+KCl$ in methanol/H_2O						
56.	Li et al. (2010)	CdS, CdSe	TiO_2	$Na_2S+S+KCl$ in methanol/H_2O	Pt	SILAR	36	1.14	CdS/CdSe core/shell QDs sensitized on TiO_2 nanowires array at optimal three cycles deposition.	[212]
57.	Liu et al. (2010)	CdS, CdSe	TiO_2	$Na_2S+S+KCl$	Pt	SILAR, CBD	41	2.05	Improved CdS/CdSe QDs co-sensitized solar cells obtained with the application of SiO_2 coating.	[126]
58.	Salant et al. (2010)	CdSe	TiO_2	Na2S+S+KOH	Pt	Electro-phoretic	35	1.70	Facile electrophoretic deposition technique for fabrication of QDSSC.	[72]
59.	Seol et al. (2010)	CdS, CdSe	ZnO	$Na_2S+S+KCl$ in methanol/H_2O	Au	CBD	38.3	4.15	QDSSC prepared by covering ZnO nanowires with CdS shell (which reduced the charge recombination) and then sensitized with CdSe QDs.	[179]
60.	Shen et al. (2010)	CdSe	TiO_2	Na_2S+S	Cu_2S	CBD	53	1.80	A low-cost CdSe QDSSC prepared without using transparent conductive glass and Pt.	[213]
61.	Yang and Chang (2010)	CdHgTe, CdTe	TiO_2	$LiI+I_2$ in EMImSCN	Pt	Linker	62	2.20	High efficiency of QDSSC incorporating CdHgTe and CdTe attributed to better electron transfer efficiency in the system.	[214]
62.	Yang et al. (2010)	CdS, CdSe	TiO_2	$Na_2S+S+KCl$ in methanol/H_2O	CoS	CBD	50.5	3.40	Low-cost CoS CE promotes the reduction action of polysulfide at the CE-electrolyte interface.	[183]
63.	Yu et al. (2010)	CdS, CdSe	TiO_2	Na_2S+S based on PAM-MBA hydrogel	Cu_2S	CBD	60.1	4.00	Improved stability of device with polysulfide electrolyte based on PAM-MBA hydrogel.	[173]
64.	Zhang et al. (2010)	CdS	TiO_2	Na_2S+S	Carbon	CBD	58	1.47	CdS-sensitized solar cells employing carbon as CE presented a higher efficiency than those with Pt CE.	[174]
65.	Zhu et al. (2010)	CdS	$Zn–TiO_2$	$Na_2S+S+KCl$ in methanol/H_2O	Au	SILAR	41	2.38	High efficiency of QDSSCs based on Zn-doped TiO_2 film photoanode, which is attributed to the reduction of electron recombination and the enhancement of electron transport.	[144]
66.	Zhu et al. (2010)	CdS	TiO_2	$Na_2S+S+KCl$ in methanol/H_2O	Au	SILAR	41	1.62	Higher efficiency of QDSSC based on Au-doped FTO attributed to the easier transport of excited electrons and the inhibition of charge recombination in the Au layer.	[145]
67.	Zhu et al. (2010)	CdS	Graphene+TiO_2	$Na_2S+S+KCl$ in methanol/H_2O	Au	SILAR	35	1.44	CdS QDSSC incorporating graphene in TiO_2 photoanode showed better efficiency than without graphene which is attributed to the enhancement of electron transport and reduction of the electron recombination.	[146]
68.	Chen et al. (2011)	CdS	ZnO	Na_2S+S	Pt	SILAR	28	1.16	High efficiency of CdS QDs-sensitized multi-layer porous ZnO nanosheets.	[215]
69.	Chen et al. (2011)	CdSe	TiO_2	$Na_2S+S+NaOH$	Pt	Linker	55.8	1.26	Improved performance of QDSSC based on two sizes of CdSe QDs (broader spectrum absorption range and longer electron lifetime).	[88]
70.	Chen et al. (2011)	CdSe	ZnO	I_2+LiI +TBP+HMII in MAN	Pt	Electro-phoretic	47.4	0.74	Fabricated flexible QDSSCs by CdSe QDs deposited on ZnO nanorods.	[216]
71.	Chen et al. (2011)	CdSe	TiO_2	CuSCN	C	Linker	–	–	CdSe QDSSC with CuSCN as solid-state electrolyte where hydrolyzate of MPTMS forms an insulating barrier layer for reduction of recombination.	[217]
72.	Chou et al. (2011)	CdS	TiO_2	$Na_2S+S+KCl$ in methanol/H_2O with GuSCN+SiO_2	Au	SILAR	50	2.01	High efficiency of QDSSC with polystyrene-modified TiO_2 film and guanidine thiocyanate (GuSCN) additive in the electrolyte.	[169]
73.	Fang et al. (2011)	CdSe	TiO_2	$Na_2S+S+KCl$ in methanol/H_2O	Carbon	CBD	60	4.81	Cell with carbon nanofibers as CE demonstrated a high catalytic activity towards the reduction of electrolyte.	[175]
74.	Greenwald et al. (2011)	CdS, CdSe	ZrO_2	$Na_2S+S+NaOH$	Pb/PbS	CBD, SILAR	63	–	A QDSSC based on a porous ZrO_2 film. Electron injection was observed from photo-excited QDs into the ZrO_2, even though with much higher conduction band edge of bulk ZrO_2.	[218]
75.	Hossain et al. (2011)	CdSe	TiO_2	Na_2S+S	Pt	CBD	49.5	1.56	Reported solar cell based on bubble-like CdSe nanocluster sensitized on TiO_2 nanotube array.	[87]
76.	Huang et al. (2011)	CdS, CdSe	TiO_2	Na_2S+S	Cu_2S	CBD	59.8	3.47	Fabrication of flexible electrode of CdS/CdSe QDSSC.	[177]
77.	Jovanovski et al. (2011)	CdSe	TiO_2	S^{2-}/S_n^{2-}-based ionic liquid	Pt	SILAR	32	1.86	First reported sulfide/polysulfide-based ionic liquid electrolyte for CdSe QDSSC.	[170]
78.	Lai and Chou (2011)	CdSe	–	Na_2S+S in methanol/H_2O	Pt	CBD	26	1.25	A facile and surfactant free CBD method.	[160]
79.	Lee et al. (2011)	CdS	TiO_2	$Na_2S+S+KCl$ in methanol/H_2O	Pt	SPD	36.3	1.71	Porous structure CdS formed by SPD for the preparation of QDSSC.	[74]

80.	Li et al. (2011)	CdS	TiO_2	Polysulfide in MPN	Pt	CBD	89	3.20	An efficient and non-corrosive polysulfide electrolyte for CdS linked to TiO_2 via TGA.	[219]
81.	Luan et al. (2011)	CdS, CdSe	ZnO	LiI+I_2+DMPII in ACN	Pt	Linker	55	~1.00	QDSSC performance based on ZnO nanorod with Al_2O_3 layer prior to QD anchoring acts as barrier inhibiting electron recombination.	[92]
82.	Qian et al. (2011)	CdS	TiO_2	P3HT in chlorobenzene	Au	SILAR	50	1.42	Improved performance of CdS QDSSC using P3HT as the hole conductor.	[172]
83.	Radich et al. (2011)	CdS, CdSe	TiO_2	Na_2S+S	Cu_2S-RGO	SILAR	46	4.40	Better fill factor obtained with QDSSC using Cu_2S-RGO composite as counter electrode.	[184]
84.	Samadpour et al. (2011)	CdSe	TiO_2	Na_2S+S+NaOH	Cu_2S	SILAR	58	3.93	Improved efficiency by fluorine treatment on photoanode.	[127]
85.	Sudhagar et al. (2011)	CdS, CdSe	TiO_2	Na_2S+S	Carbon	CBD	50	1.75	High efficiency of QDSSC using mesocellular carbon foam as CE due to enhanced catalytic activity.	[176]
86.	Sun et al. (2011)	CdSe	Graphene	LiI+I_2+TBP in ACN	Pt	CBD	36.9	0.76	Graphene network as conducting scaffold to capture and transport photoinduced charge carriers.	[220]
87.	Yeh et al. (2011)	CdS	TiO_2	Na_2S+S+KCl in methanol/H_2O	PEDOT	SILAR	50	1.35	High efficiency QDSSC due to high electrocatalytic activity of PEDOT as CE.	[185]
88.	Yu et al. (2011)	CdS, CdTe	TiO_2	Na_2S+S+NaOH in methanol/H_2O	Au	Linker+CBD	41	3.80	High efficiency of CdTe/CdS QDSSCs prepared by linker assisted CBD.	[180]
89.	Zeng et al. (2011)	CdS	TiO_2	Na_2S+S	Pt	CBD	47	1.27	Fabrication of CdS QDSSC using free-standing single-crystalline rutile TiO_2 nanorod arrays.	[135]
90.	Zewdu et al. (2011)	CdS, CdSe	TiO_2	Na_2S+S+KCl in methanol/H_2O	Au	SILAR	~50	3.60	Transient absorption spectroscopy data in the presence of the polysulfide electrolyte indicated regeneration not as efficient as cell using dye sensitizer and iodide based redox couple.	[181]
91.	Zhang et al. (2011)	CdS, CdSe	TiO_2	Na_2S+S	Cu_2S	CBD	63	4.92	Introduction of large size TiO_2 particles into the photoanode for wider pore size distribution as in double-layer photoanodic structure.	[153]
92.	Zhu et al. (2011)	CdS	ZnO	Na_2S+S+KCl in methanol/H_2O	Au	SPD	33	1.54	Efficient CdS QDSSC based on ZnO photoanode fabricated by using ultrasonic spray pyrolysis.	[75]
93.	Zhu et al. (2011)	CdS	TiO_2	Na_2S+S+KCl in methanol/H_2O	Au	CBD – microwave assisted	38	1.03	Improved short circuit current density and efficiency in QDSSC with QDs prepared using microwave assisted CBD.	[61]
94.	Zhu et al. (2011)	CdS	TiO_2, ZnO	Na_2S+S+KCl in methanol/H_2O	Au	SILAR	35	1.56	Reduction of charge recombination by ZnO passivation layer in QDSSC based on cascade structure of TiO_2/ZnO/CdS.	[152]
95.	Zhu et al. (2011)	CdS, CdSe	TiO_2	Na_2S+S+KCl in methanol/H_2O	Pt	Microwave-assisted CBD	33.7	3.06	Direct and rapid deposition of QDs with good contact forming between QDs and TiO_2 films via microwave-assisted CBD.	[62]
96.	Barcelo et al. (2012)	CdSe	TiO_2	Quaterthiophene	pTPA	DA	–	0.34	DA CdSe electrode yields better result with high V_{OC} using quarterthiophene hole conductor.	[221]
97.	Cheng et al. (2012)	CdS, CdSe	TiO_2	Na_2S+Na_2SO_3	Pt	SILAR	58	2.41	High performance of CdS/CdSe-sensitized solar cell using TiO_2 nanotubes with nanowires.	[99]
98.	Hossain et al. (2012)	CdS, CdSe	TiO_2	Na_2S+S+NaOH	Cu_2S	SILAR	57	5.21	The presence of CdS buffer layer impeded the injection of electrons from CdSe to TiO_2 and accelerates charge recombination at the TiO_2/sensitizer interface. Obtained high efficiency with scattering layer in CdSe QDSSC.	[155]
99.	Jang et al. (2012)	CdS	TiO_2	Na_2S+S+KCl in methanol/H_2O	Pt	SILAR	43	1.33	Used liquid CO_2 coating for deposition of CdS QDs on mesoporous TiO_2 films. CdS QDs were uniformly deposited throughout TiO_2 film.	[222]
100.	Jung et al. (2012)	CdS	TiO_2	Na_2S+S+KCl in methanol/H_2O	Pt	SILAR	44.8	1.72	Improvement of CdS QDSSC by ZnS overlayers which act as efficient energy barrier at interface, leading to the supression of recombination from the large CdS QD to the electrolyte.	[223]
101.	Lai et al. (2012)	CdS, CdSe	TiO_2	Na_2S+S+KCl in methanol/H_2O	Pt	SILAR, CBD	33	2.74	Improved QDSSC with annealed TiO_2 nanotube arrays.	[224]
102.	Ning et al. (2012)	CdS, ZnSe	TiO_2	Thiourea-based organic redox couple	Pt	Linker	58	0.86	Core/shell ZnSe/CdS type-II QDs give higher electron injection than CdS/ZnSe QDs in QDSSC using a organic based electrolyte.	[225]
103.	Rawal et al. (2012)	CdS, CdSe	ZnO	Na_2S+S+KCl in methanol/H_2O	Pt	CBD	37	1.33	Highly uniform film-like structure of deposited CdS on ZnO nanorods for the application in CdS/CdSe QDSSC.	[226]
104.	Salant et al. (2012)	CdSe	TiO_2	Polysulfide	PbS	Electro-phoretic	49	2.70	Higher performance of quantum rod-sensitized solar cell compared to the usual QDSSC.	[227]
105.	Santra and Kamat (2012)	CdS, CdSe	TiO_2	Na_2S+S	Cu_2S - RGO	SILAR	47	5.42	Highest efficiency reported to date with Mn-doped-CdS/CdSe QDSSC.	[112]
106.	Shu et al. (2012)	$CdSe_xS_{(1-x)}$, CdSe	TiO_2	Na_2S+S+KCl in methanol/H_2O	Pt	SILAR	64	3.67	QDSSC with nitrogen-doped TiO_2 spheres showed improved performance due to efficient electron transport, higher QD loading and enhanced light scattering.	[151]

Table 1 (*continued*)

No.	Author	Sensitizer	Wide band gap semiconductor	Electrolyte*	Counter electrode	QD deposition method	FF (%)	η (%)	Highlights	Ref.
107.	Song et al. (2012)	CdSe	TiO_2	$Na_2S+S+KCl$ in methanol/H_2O	Pt	Linker	33.8	1.97	In situ hydrothermal method to assemble aqueous TGA-capped CdSe QDs onto TiO_2 films with better control over QD size.	[228]
108.	Tian et al. (2012)	CdS, CdSe	TiO_2	Na_2S+S	Cu_2S	SILAR, CBD	55	4.62	Optimum TiO_2 film thickness of 11 μm produced the highest efficiency.	[154]
109.	Wang et al. (2012)	CdSe	TiO_2	$Na_2S+S+NaOH$	Cu_2S	Linker	46	2.21	In situ deposition method to directly assemble aqueous TGA capped CdSe colloidal QDs within TiO_2 films by a low-temperature hydrothermal route.	[229]
110.	Wang et al. (2012)	CdS	TiO_2	$Na_2S+S+KCl$ in methanol/H_2O	Pt	SILAR	–	2.54	High efficiency CdS QDSSC with CdS QD deposited onto TiO_2 nanorod using ultrasound assisted SILAR.	[136]
111.	Yu et al. (2012)	CdS, CdSe	TiO_2	$Na_2S+S+KCl$ in methanol/H_2O	Cu_2S	Linker-assisted CBD	55	4.21	High efficiency obtained in a QDSSC with co-sensitization of CdS, CdSe and ZnS layer and annealed at 400°C.	[129]
112.	Zhang et al. (2012)	CdS, CdSe	TiO_2	$Na_2S+S+KCl$ in methanol/H_2O	Pt	SILAR	47	2.26	Higher deposition cycles of CdSe has a negative effect for the generation and collection of photoelectron while higher amount of CdS and CdSe caused a downward displacement of TiO_2 CB.	[230]
113	Zhang et al. (2012)	CdS, CdSe	TiO_2	Na_2S+S	Cu_2S	CBD	62	4.61	Highly efficient CdS/CdSe QDSSC with $TiCl_4$ treated TiO_2 nanotubes array. TiO_2 nanotubes were fabricated by sol–gel assisted template process.	[156]
114.	Zhao et al. (2012)	CdSe	TiO_2	$Na_2S+S+KCl$ in methanol/H_2O	Pt	CBD	49.4	2.13	Improved performance of CdSe QDSSC by $TiCl_4$ treatment of QD-sensitized electrode.	[157]

* *Note*: Electrolytes are aqueous solutions unless otherwise stated.
[a] Value is for CdS QDSSC at 9.4% sun intensity.

CdS deposited TiO_2 layer, and the electrode was subsequently pressed between two plates. The photoanode prepared via the pressing route has a tendency of experiencing partial loss or damage of the CdS layer. This method may also create regions that are inaccessible to the redox electrolyte. Nevertheless, the pressing route according to the authors gives an alternative low cost method for the preparation of QD-sensitized photoelectrodes.

Electrophoretic deposition, a new deposition technique which was used recently by Salant et al. [72] in 2010 has been able to generate high power conversion efficiency in CdSe-sensitized QDSSCs. The reported efficiency of 1.7% at 1 sun was higher than those of the cells with QDs prepared with a linker technique. Interestingly, the absorbed photon to electron conversion efficiencies is not size dependent, which means that efficient electron injection can take place for larger QD sizes. Poulose et al. [73] in 2012 have adopted a combination method of functional linker with electrophoretic deposition to fabricate CdSe QDs. This method has the advantage of obtaining better QD deposition onto TiO_2 layers with reduced deposition time. This opens an alternative route for efficient QD deposition.

QDs can also be prepared via spray pyrolysis deposition (SPD) [74–76]. In the case of a CdS QDSSC reported by Lee et al., CdS QD was deposited onto the TiO_2 layer via SPD using solution mixture of cadmium chloride and thiourea [74]. The deposited CdS layer had a porous structure. The photoelectrode was then subjected to washing to remove the excess cadmium chloride. The performance of the QDSSC prepared by this technique is comparable with those of the cells prepared by other existing techniques. The performance was mainly attributed to the large surface area of the formed CdS in contact with the electrolyte. As high temperature of the order of above 400 °C is required and the performance of QDSSCs is also not improved very much, this method is not used by many researchers. Other new alternative methods include electro-spray technique and spin-coating-based SILAR [77,78]. In electro-spray technique, QDs suspension is prepared and loaded in a syringe. A syringe pump feed the suspension through the needle at a constant flow rate. High voltage is applied to the needle so that a cone-jet is formed at the needle outlet. QDs suspension is then sprayed onto the TiO_2 film which is set perpendicular to the needle. This method is very similar to the electro-spinning method. In spin-coating-based SILAR, both anionic and cationic precursors are dropped onto the TiO_2 film surface. The sample is then spin-coated without rinsing and drying process. This process is repeated few times until a desired QD layer is formed. Spin-coating-based method proves to be simple and fast as compared with normal SILAR method. However, much optimization work is needed to obtain a comparable cell performance with the cell containing QDs prepared from normal SILAR method.

5. Approaches for improving QDSSC performance

In view of the low energy conversion efficiency achieved by Cd chalcogenide QDSSCs (largely below 5%), a systematic approach is needed to modify the architecture of the QDSSC assembly for a better efficiency yield. The main approaches that most of the researchers focused on are materials selection and materials engineering. This covers the types of QD material used and their sizes, choices of electron conductor for photoanode, counter electrode materials, electrolyte, and the surface engineering of the materials. In this review, more than 150 articles pertaining to Cd chalcogenide QDSSCs have been reviewed. Some of the significant results and reports from these articles are summarized in Table 1 for quick and easy comparison among the QDSSCs that have been reported. The list displayed in Table 1 is by no means

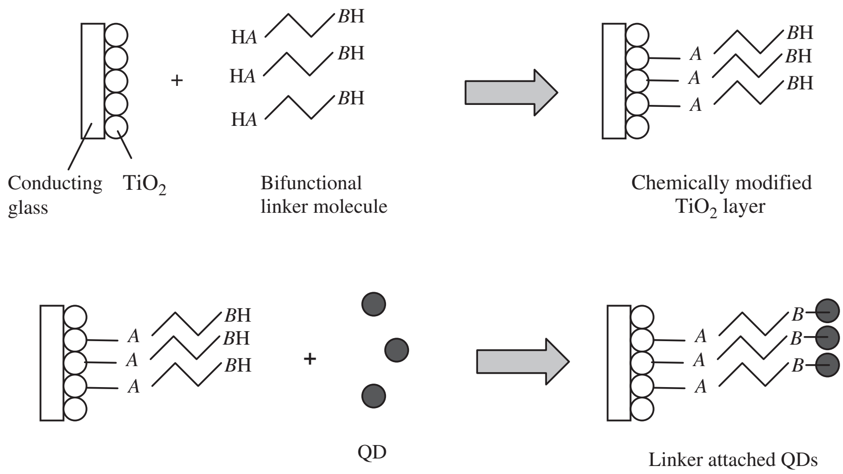


Fig. 8. Linking QDs to TiO_2 surface with a bifunctional molecular linker.

exhaustive. The following sections discuss some of the notable results pertaining to improving QDSSCs performance.

5.1. Type of QD sensitizers and their sizes

QDs employed in QDSSCs as sensitizers include but not limited to $CuInS_2$ [79], PbS [80], InP [32], InAs [81], Ag_2S [82,83], CdS [64], CdSe [33], CdTe [84] and ZnSe [85]. Among these, Cd chalcogenide QDs have been considered as a better choice as they are more stable in QDSSCs although they may degrade upon visible illumination [86]. However, the degradation is not as severe as PbS QDs. CdS QDs are reported to be relatively more stable.

By engineering the morphology of the QD surface, there is a possibility of gaining ground breaking improvement in photovoltaic performance. One example is the sensitization of the TiO_2 layer with bubble-like QDs. Hossain et al. have used the CBD method to fabricate such CdSe QDs and used them to obtain an efficiency of 1.56% in a QDSSC arrangement. [87]. In their work, the improvement observed in the performance of the cell was mainly attributed to the increase in the size of the QDs and the surface area covered by them on the photoelectrode. Furthermore, the nanotube form of the TiO_2 enabled more QDs coverage. The performance of the cell containing bubble like QDs on such nanotubes (efficiency of 1.56%) was reported to be better compared to the QDSSC using TiO_2 nanotube structure with the usual QDs deposition.

On the other hand, QDSSCs prepared with two or more sizes of QDs can improve the cell performance as the I_{sc} and fill factor are expected to be significantly enhanced. The use of two different sizes of CdSe QDs has shown an improved performance compared to that of a cell with a single sized QDs. Chen et al. [88] have used two different sizes of CdSe QDs in a QDSSC. The combination of 2.5 nm and 3.5 nm QDs in a CdSe QDCC produced an efficiency of 1.26% where as the efficiency of the cell with QDs of single size was below 1%. This improvement in the former cell may have been due to broader light absorption range as well as longer electron lifetime. It could also be deduced that charge recombination at the interface is minimized with the application of two or more sizes of CdSe QDs.

Another approach to improve QDSSCs performance is to couple several QD nanoparticles to form a core/shell structure. Coupling two types of nanoparticles as core/shell or multi shell structure can increase the photoelectrochecmical performance remarkably as compared with bare nanoparticle QDs. This was shown in Sung et al. [89] work in which they have fabricated QDSSC using $CdS_xSe_{(1-x)}$ as QDs with core/shell structure. As the ratio of Se was increased in the multi shell structure of CdS/CdSSe/CdSe, higher photocurrent density was observed in QDSSCs made with them. In another example, QDSSCs formed with CdSe/CdS core/shell nanocrystals were found to produce superior performance in comparison to the QDSSCs with highly luminescent CdSe plain core nanocrystals as reported by Li et al. [90]. With CdSe/CdS core/shell structure, improvement in photoluminescence quantum yield was observed. Improvements in short-circuit current density were also observed in CdTe/CdS and CdS/CdSe core/shell solar cell structures [91–93]. Hence, it can be concluded that one type of QDs alone cannot bring up the energy conversion efficiency of QDSSCs to a higher level. The improvement is also influenced by the choice of semiconductor material, core size and shell thickness. Dworak et al. reported that, through the observation from femtosecond absorption spectroscopy, the rate of the interfacial electron transfer reaction depends on CdS shell thickness. With lower CdS shell thickness, the transfer rate is better [94].

A thin coating of amorphous TiO_2 mesoporous layer on the CdS QD layer can improve the performance and photostability of the QDSSCs as shown in Shalom et al.'s work [95]. The TiO_2 coating layer actually assists in passivating the QD surface state and reduces the recombination of electrons from the QDs and TiO_2 into the electrolyte solution. Shalom et al. reported an efficiency of 1.24% in a CdS QDSSC with an amorphous TiO_2 coating on the QDs compared to 0.13% without this coating, an increase of more than 900%. It is also interesting to note that the cell was tested with iodine/iodide electrolyte instead of the usual polysulfide electrolyte. When coupled with other QDs, Cd chalcogenide can serve as a coating layer as well as a stabilizer for the solar cell behavior. This was demonstrated in PbS QDSSCs employing a CdS coating layer [96]. With CdS coating the PbS QD, the observed photocurrent density in a QDSSC increased from 4 mA cm^{-2} to 11 mA cm^{-2}, a 175% increase. The efficiency of the cell with the CdS coating was 2.21% under 1 sun. The CdS QDs light-absorbing layer also acts as a blocking layer for reducing the recombination in QDSSCs. Essentially, the CdS coating expands the absorption spectra of the QDs while scavenging the photogenerated holes in the valence band of the QDs in order to promote the charge separation [97]. Lately, better results reported on QDSSCs prepared using multilayered QDs structure. In Lee et al.'s [98] work, multilayered QDs of CdS/CdSe/ZnS were fabricated using the SILAR method. The highest QDSSC efficiency achieved was 3.90% using this arrangement. This performance is far better than that of the cell with a single QD layer arrangement which gave efficiencies of only 0.48% and 2.23% for CdS and CdSe QDSSC respectively. The improved performance is attributed to the enhanced charge separation at the main absorbing QD layer as a result of addition of under layers and over layers to the main absorbing QD layer. In another development,

Cheng et al. have developed multilayered QDs of CdS/CdSe/ZnS to sensitize TiO_2 in the form of nanowires [99]. Although the efficiency obtained (2.41%) is not as high as in Lee et al.'s work, their concept could pave way for a possible further improvement due to high surface area of the TiO_2 nanowires.

Dye sensitizers used in DSSC could lift up the solar cell performance when coupled with QDs sensitizers. Improvement of electron extraction from QDs into the wide band gap semiconductor was observed when N3 dye was deposited on top of the QDs layer [100,101]. This is due to efficient hole transfer from the valence band of the excited QDs to the ground state of the N3 dye molecules which yields improvement in the cell performance and stability. Beside the N3 dye, Fan et al. [102] have showed that co-sensitizing the TiO_2 layer with CdSe QDs and other organic dyes is able to yield improvement on the cell performance too. However, the cell performance is still lagging behind that of the best DSSC system reported. Nevertheless, this approach opens up an alternative way for new solar cell design. Other notable works are coupling QDs with near-infrared red absorbing dye for panchromatic harvesting light system [103,104]. Such co-sensitization with CdS QD and squariand dye has yielded an efficiency of 3.14% in a QDSSC [104]. Other examples of coupling QDs and dye for co-sensitization in solar cells which give higher power conversion efficiencies have also been reported in the recent literature [105–107]. Lee et al. [106] have reported an excellent performance with 4.76% efficiency in a QDSSC with co-sensitizers of CdSe and Z907Na dye on the TiO_2 film. The team has used cobalt-based electrolyte which could have been another reason for the better performance and stability of the cell. Meanwhile, Ling et al. [108] have demonstrated a hybrid-sensitized solar cell consisting of TiO_2 spongy structure sensitized with CdS and N3 dye. There was a 100% increase in efficiency in the co-sensitized device compared with that of the CdS QDSSC. The light conversion process is enhanced with the modified porous architecture of TiO_2 and through improved penetration of the electrolyte into the photoanode. In another development, Shalom et al. [109] have showed a new co-sensitization structure with the application of an amorphous TiO_2 layer between the QD and dye layers. Utilizing such two sensitizing layers, the team observed a 250% increase in efficiency compared to that of a QD monolayer cell.

The use of functional linkers to attach QD sensitizers plays an important role which affects the end result of the solar cell performance [70,110]. Mora-Seo et al. [110] have reported a 5–6 fold increase in IPCE value with the use of cysteine as a functional linker between CdSe QDs and TiO_2 layer. Even the pH condition of the chemical solution used during QD loading with functional linkers can also play a role in determining QDSSCs' performance [40,111]. Under an optimum pH value of the solution, large loading and better coverage of QDs on the wide band gap semiconductor film can be realized which eventually yield a better efficiency and IPCE value. Chen et al. [111] have reported that higher loading and good QD coverage on TiO_2 was obtained in study with optimal pH value of 7.

Most recently, Santra et al. have fabricated a high efficiency QDSSC with Mn doping. They have obtained a cell efficiency of 5.42% using Mn-doped-CdS/CdSe QDs. This is by far the highest efficiency reported for Cd chalcogenide QDSSCs [112]. In this structure, Mn dopant creates an electronic state in the midgap region of the CdS/CdSe QD. In other words, there is a midgap level within the main QD band gap. This midgap state acts as an electron trap and prevents charge recombination with holes and/or oxidized electrolyte. Further study is needed to understand the structure of this QDSSC towards performance improvement.

5.2. Type and surface morphology of the working electrode

The preparation route of QDs plays an important role in QDSSCs as it indirectly affects the final outcome of the solar cell performance. As discussed in Section 4, each QD fabrication route yields a different range of performance although there is no specific range applicable to each fabrication method. It is also noted that the surface state of QDs contribute to the density of states distribution which suggests that QDs have a significant role in the recombination process [113]. Therefore, optimization should consider the QD arrangement and the surface states which depend on the QD fabrication process and surface treatment.

QDs prepared in situ by CBD process has significantly higher QDs loading on photoanodes. Nevertheless the maximum efficiency achieved by CBD processed QDs is only 10% higher than that obtained with pre-synthesized QDs (DA or linker attachment) [114,115]. In a recent work by Guijarro et al. [116], QDSSCs based on colloids (DA, linker attachment) have the potential of being superior to those prepared by CBD or SILAR as faster recombination was observed in the latter case. Recombination of electron from the photoanode to electrolyte is not desirable. Therefore, a delayed or reduced recombination rate is favorable. When comparing between DA and linker attachment, faster electron injection from QDs into TiO_2 layer was observed in QDs deposited by DA [117]. Thus, larger photocurrent is expected for DA processed QDs.

In the SILAR process, every additional dipping cycle will increase the size of the QD layers on the photoanode. The QD size for optimum QDSSC performance is usually reached with few dipping cycles. SILAR deposition appears to give better QD distribution throughout the TiO_2 layer. This is possible due to easy access of ionic precursors to the deeper regions of the film. However, the rate of the photogenerated electron injection from the QDs to the wide band gap semiconductor decreases with the additional deposition cycles [116]. As such, the efficiency gets saturated as the number of SILAR cycle increases. This is justified by the saturation of the QDs on the oxide surface as the deposition cycles are increased. The excessive layers will then become blocking layers instead.

In linker assisted attachment of QDs, different linkers affect the electron injection and/or recombination at the QD/electrolyte interface. For example, the influence of cysteine adsorption on the performance of CdSe QDSSC has been reported by Xu et al. [118]. Electron recombination at the interface between the photoanode and electrolyte has been found to reduce with a large amount of adsorbed cysteine on the TiO_2 electrode's surface.

In general, QDs produced by CBD appear to give higher cell performance than the ODs produced with SILAR technique. The open-circuit voltage appears to be higher as reported by Samadpour et al. [119]. This is due to higher recombination resistance for electrodes sensitized using the CBD method. However, the SILAR method has the advantage of covering large areas in electrodes having ordered TiO_2 nanostructures. Thus, for high surface area structure such as TiO_2 nanotubes, the SILAR method should be considered. The limitation of the photoanodes prepared by SILAR can be mitigated by effective passivation of the photoanode surface.

Ruhle et al. [120] have showed the importance of suppressing the recombination at the photoanode with a compact TiO_2 layer on the ITO/FTO surface. With the presence of such a compact TiO_2 layer, the efficiency of CdSe QDSSC increased to almost 100%, depending on the compact layer thickness. Similar improvement was also observed in a CdS QDSSC when a compact TiO_2 layer was present between the conducting glass and mesoporous TiO_2 film [121]. Coating QDs with a protective ZnS layer has been showed to be capable of preventing electron leakage from the QDs into the electrolyte (in other words, it suppresses the charge recombination at the QD–electrolyte interface) [122–124]. In most QDSSCs, QDs coated with ZnS layer showed an improvement in efficiencies of at least 60% compared to the efficiencies obtained with non-passivated QDs (0.9%–1.5% in Diguna et al.'s work [122]; 1.4%–

2.9% in Lee et al.'s work [123]; 1.12%–2.02% in Shen et al.'s work [124]). In another recent work by Guijarro et al., the ZnS layer has induced the passivation of the CdSe QDs which led to the efficiency improvement [125]. This was evidenced by the increase of charge transfer resistance (related to recombination rate) and the ultrafast carrier dynamics study. These results indicate the use of both compact TiO_2 layer and ZnS passivation layer is essential in the fabrication of efficient QDSSCs.

On the other hand, coating the QD-sensitized TiO_2 surface with a SiO_2 layer gives better performance due to suppression of electron back transfer from TiO_2 to the electrolyte. The efficiency of a QDSSC increased from 1.05% to 2.05% after coating QDs with a SiO_2 layer [126]. Apparently, the SiO_2 layer plays a similar role as the ZnS passivation layer. An Al_2O_3 layer also can act as an inhibitor for electron recombination at the QD–electrolyte interface as reported by Luan et al. [92]. Besides coating with a passivation layer, surface treatment of the TiO_2 film with ionic solution helps to enhance the performance of the solar cell as well. When TiO_2 electrodes were treated with fluorine (either with NH_4F or HF), increase in power conversion efficiencies of Cd chalcogenide QDSSCs were observed [122,127]. Efficiencies as high as 1.54% and 3.93% have been obtained for CdS and CdSe QDSSC respectively for fluorine treated photoanode as observed by Samadpour et al. [127]. This enhancement is attributed to the reduction of the recombination of photoinduced carriers after fluorine treatment.

Suitable post-treatment used in synthesis and attachment of QDs also plays an important role in determining the solar cell performance. In Tena-Zaera et al.'s work, heat treatment above 350 °C on ZnO/CdSe core/shell nanowire arrays has induced a structural change in nanocrystalline CdSe [128]. The CdSe QDs also became larger after the heat treatment which might have promoted easy charge carrier injection from CdSe as evidenced by the observed increase in external quantum efficiency. Yu et al. have also reported the effect of annealing of QDs on the performance of QDSSCs [129]. A remarkable efficiency of 4.21% under 1 sun illumination was obtained with a TiO_2/CdSe/CdS/ZnS photoanode annealed at 400 °C. The cell made with the same photoanode without the heat treatment yielded an efficiency of 3.20% only.

Besides QD preparation methods, other factor that can influence the solar cell performance is the surface morphology of the photoanode particularly that of the wide band gap semiconductor or other conducting materials. Farrow et al. [130] have reported that the use of stacked-cup carbon nanotubes has produced a 10-fold increase in the photocurrent. The improvement of photocurrent is attributed to the fast electron transport between CdSe QDs and stacked-cup carbon nanotubes. With smaller CdSe QD size, electron transport is further increased making the structure a promising architecture for high efficiency light harvesting. Other notable surface morphology or "nano-geometry" reported includes TiO_2 nanofibres as in flower-like structure [131], TiO_2 nanorods [132–137], and TiO_2 nanowires [138]. All these special geometries show higher efficiencies when compared with the usual mesoporous TiO_2 film layers. For example, in Wang et al.'s work, they observed an efficiency of 2.54% in CdS QDSSC using TiO_2 nanorods compared to 1.84% of CdS QDSSC with conventional TiO_2 films [136]. Yu and Chen have reviewed the role of nanostructures geometry in enhancing the performance of solar cell [139]. They have concluded that the use of one-dimensional nanomaterials (nanotubes, nanowires and nanorods) is a good technique for improving QDSSC performance.

It is noted that different types of wide band gap semiconductor materials can produce different photovoltaic performances. Among the semiconductor materials used as electron conductors, TiO_2, ZnO and SnO_2 are popular. Other alternative materials are being investigated nowadays. In Chen et al.'s work, a new type of QDSSC based on vertically aligned carbon nanotubes arrays (CNT) coated with ZnO nanorods has been fabricated that produced a higher power conversion efficiency [140]. The CNT/ZnO/CdSe photoanode has produced 40% improvement in efficiency compared that observed with the photoanode without CNT. The use of indium tin oxide (ITO) itself as a mesoporous conductor layer also proved to be functional when sensitized with CdS QDs [141]. However, not every type of materials can serve as an optimal electron conductor. In a recent report the CdS QD-sensitized Zn_2SnO_4 porous electrode did not produce high efficiency in QDSSC arrangement [142]. The highest efficiency obtained was below 1%.

Apart from utilizing different surface morphology, hybrid materials for the electron conductor are also favored. In Liu et al.'s work, hybrid mesoporous of CdSe/TiO_2 has been demonstrated to have better photoelectrochemical properties due to the enhanced interfacial coupling between CdSe and TiO_2 [143]. The CdSe/TiO_2 hybrid mesoporous structure was formed through emulsion-based bottom-up self assembly in which CdSe QDs and TiO_2 nanoparticles were mixed together and then assembled into colloidal spheres. Then the capping ligands were removed using calcination. This resulted in strong binding between CdSe QDs and TiO_2 nanoparticles. Doping is another way for creating hybrid structure. In a CdS QDSSC employing Zn-doped nanocrystalline TiO_2 films as reported by Zhu et al. [144] a photovoltaic efficiency of more than 2% was obtained. The 24% improvement in efficiency compared to that of the CdS QDSSC with TiO_2 layer only was due to the reduction of photogenerated electron recombination. In a recent development, the use of Au or graphene as an interfacial layer between TiO_2 and QDs in a QDSSC has showed an improved power conversion efficiency compared to that in cell without Au or graphene layer [145–148]. Lightcap et al. have reported that incorporation of graphene oxide or reduced graphene oxide in colloidal CdSe QD films deposited on conducting glass electrode has improved the charge separation and electron conduction by 150% [148]. In a separate work by Liu et al., Au/TiO_2 hybrid mesoporous films seemed to enhance the IPCE data of the CdSe QDSSC by 50% [149]. Nitrogen-doped TiO_2 layer is another doping strategy for performance improvement as demonstrated by Shu et al. with a high efficiency result of 3.67% in a CdSeS/CdSe QDSSC [150,151]. Additionally, cascading two types of wide band gap semiconductor appears to pave an alternative way for performance enhancement as in the case of QDSSC based on cascade structure of TiO_2/ZnO/CdS electrode [152]. The cascade structure showed an improvement in efficiency of more than 50% compared to that of the QDSSC with TiO_2/CdS electrode.

By varying the thickness or particle size of the TiO_2 layer, high energy conversion efficiencies can be achieved. This has been demonstrated by Zhang et al. [153] with a double-layer TiO_2 photoanodic structure having larger size of TiO_2 nanoparticles giving an energy conversion efficiency of 4.92%. The high efficiency was also attributed to the optimized thickness of TiO_2 layer. An optimum TiO_2 film thickness of 11 μm could produce high cell efficiency for Cd chalcogenide QDSSC as reported by Tian et al. They obtained an efficiency of 4.62% [154]. Applying a scattering layer on top of the TiO_2film as practised in DSSCs also helps to improve the QDSSC performance to some degree. This has been shown by Hossain et al. by obtaining an efficiency of 5.21% with a scattering layer in a CdSe QDSSC [155]. More recently, few groups of researchers have shown asignificant contribution of $TiCl_4$ treated TiO_2 towards improving the QDSSC performance [156–158]. Zhang et al. have observed an efficiency of 4.61% in a CdS/CdSe QDSSC having $TiCl_4$ treated TiO_2 nanotubes array. This technique which was previously used in DSSC applications has become a good strategy in improving QDSSC performance.

Nevertheless, there are other methods which may not give higher power conversion efficiencies but have the potential for providing further improvement in the performance of QDSSCs. One such approach is mesoporous TiO_2 films prepared on conductive glass using a copolymer as template [159]. Another alternative method is depositing QDs right on the transparent conducting glass without the wide band gap semiconductor layer. Such an approach though is unusual, gives modest power conversion efficiency around 1% [160]. Besides these developments, investigation is under way to identify alternative cost effective substrates for the photoelectrode. Recent research has identified steel substrate as a potential candidate [161]. However, further optimization is needed to enhance its photovoltaic performance.

5.3. Stability—the role of electrolytes/redox mediator

In DSSCs, iodide/triodide based liquid electrolytes are commonly used as redox mediators [21]. However, the use of iodide based electrolyte does not give good performance in Cd chalcogenide QDSSCs. The efficiency is usually very poor – less than 1% [162]. This is because iodide based electrolyte itself is corrosive towards the Cd chalcogenide QDs, especially for CdTe QDSSCs [163]. To remedy this problem, one should improve the surface morpohology of the photoanode by applying a passive coating (as explained in Section 5.2) or use other non-corrosive type electrolytes.

Recent developments have seen the use of cobalt based electrolyte which promises high efficiency in QDSSCs [65,106,164,165]. Cobalt based electrolyte is also suitable to be used in DSSCs. As such, solar cells with co-sensitizers of QD and dye can use cobalt based electrolytes as common redox mediators. An efficiency as high as 4.76% has been achieved in a QDSSC based on cobalt redox couple as reported by Lee et al. [106]. This has placed cobalt redox couple as the most superior redox mediator for QDSSCs thus far.

For Cd chalcogenide QDSSCs, the commonly used electrolyte is polysulfide based [115,166]. However, not all QD sensitizers benefit from the usage of polysulfide electrolytes. Nevertheless, the presence of polysulfide electrolyte is imperative for the stability of metal chalcogenide-based QDSSCs. Bang and Kamat revealed that the sulfide ions are only capable of scavenging photogenerated holes in photoirradiated CdSe QDs system and not in CdTe QDs system [167]. However, in a recent work it was suggested that there is a slow hole scavenging from CdSe by sulfide ions which hinders the high overall efficiency [168]. As a result, the electrons aggregated within the TiO_2 matrix are prone to recombination at the interface between the photoanode and electrolyte, which in turn constrain the photocurrent generation efficiency. With the presence of the oxidized couple (i.e. addition of S or Se to the electrolyte), the rate of back electron transfer is further elevated. As such, a better way to control the back electron transfer is by surface modification of the QDs such as passivation layer coating.

Inclusion of additives to the electrolyte can give rise to better photoelectrochemical performance too. One example is guanidine thiocyanate (GuSCN) which has been shown to be a good additive for the polysulfide electrolyte as reported by Chou et al. [169]. The group obtained an efficiency of 2.01% in CdS QDSSC using GuSCN added polysulfide electrolyte. The efficiency is better than that of the previous reported CdS QDSSC having only polysulfide electrolyte [16]. The cells also showed a better stability of polysulfide electrolyte with the addition of SiO_2 nanoparticles. Ionic liquid which is commonly used in DSSC also has been demonstrated by Jovanovki et al. to be compatible in QDSSCs [170]. They obtained a cell efficiency of 1.86% with a high short-circuit photocurrent of 14 mA cm^{-2} in a CdSe QDSSC having the new pyrrolidinium ionic liquid. However, further optimization is needed to bring up the performance of the cell to match with that of the cells having cobalt based or polysulfide electrolytes.

One particular solar cell property that has been attracting the attention from researchers is the internal quantum efficiency (IQE). IQE represents the efficiency rate of the absorbed photons that are converted to current in the external circuit. IQE can achieve the ideal value of 1 (or 100%). This has been successfully demonstrated by Fuke et al. by employing a Li_2S electrolyte [171]. This result opens a new direction for experimenting more efficient electrolytes for QDSSCs.

As liquid electrolytes do not give outstanding long term stability to QDSSCs, a suitable solid-state electrolyte is necessary to be developed to meet the stability requirement. Among the materials that have been developed to meet this criterion include but not limited to spiro-OMeTAD [65] and poly(3-hexylthiophene) (P3HT) which are hole conductors [168,172]. The use of P3HT has produced a better performance in a CdS QDSSC compared to those of cells using I^-/I_3^- or S^{2-}/S_x based electrolytes [172]. P3HT has produced an efficiency of 1.42% which is comparable to the efficiencies of the usual CdS QDSSCs with polysulfide liquid electrolytes. One notable discovery reported recently is the high efficiency quasi-solid-state QDSSC based on hydrogel electrolytes by Yu et al. [173]. The CdS/CdSe QDSSC with a polysulfide electrolyte based on PAM-MBA hydrogel achieved power conversion efficiency up to 4.0%. Unless a major breakthrough is made in developing an efficient electrolyte system, researchers have to rely on cobalt based or polysulfide electrolyte for their Cd chalcogenide based QDSSCs.

5.4. Effect of different counter electrodes

Different counter electrodes (CEs) employed in Cd chalcogenide QDSSCs can affect their overall performance [69]. In general, platinized transparent conductor layers have been used in most QDSSC assemblies. The Pt CE has been used in more than 50% of the Cd chalcogenide QDSSCs reported (refer to Table 1). However, there are other materials which have shown better performance in QDSSCs when used as CEs. Notable alternative materials for CEs include carbon, Au, Cu_2S and reduced graphene oxide.

Carbon is an alternative candidate for CEs due to its corrosion-inertness towards the polysulfide redox couple [174]. Application of carbon as a CE has enabled the fabrication of high-efficiency QDSSCs. Coupled with nanofibers geometry, efficiency of up to 4.81% has been achieved in a CdSe QDSSC as reported by Fang et al. [175]. In Sudhagar et al.'s work, CE with modified surface morphology like mesocellular carbon foam has enhanced the performance of CdS/CdSe QDSSCs [176]. The cell with this CE has produced an efficiency of 1.75% where as QDSSC using Pt as CE had an efficiency of 1.22%. The increased performance is attributed to the enhanced catalytic activity of the CE due to the large pores and surface area of the carbon foam. Nevertheless, more optimization and improvement are needed to achieve better efficiencies in Cd chalcogenide QDSSCs employing carbon as CEs.

Cu_2S is another preferred choice for CEs. In recent studies, higher efficiencies for Cd chalcogenide QDSSCs were obtained with Cu_2S as CEs [173,177]. Generally, Cu_2S CE is prepared from brass sheet by reacting it with concentrated HCl followed by dipping into an aqueous polysulfide solution. The highest efficiency of 5.21% has been obtained in a Cd chalcogenide QDSSC with Cu_2S as the CE by Hossain et al. [155]. A better CE material for QDSSCs is Au due to its inertness. Cd chalcogenide QDSSCs utilizing Au as CE have shown better performances compared to those of the cells with Pt as the CE [93,144,145,169,172,178–181]. To date, the highest cell efficiency reported for Cd chalcogenide QDSSC using Au as the CE is 4.22% by Lee et al. [93].

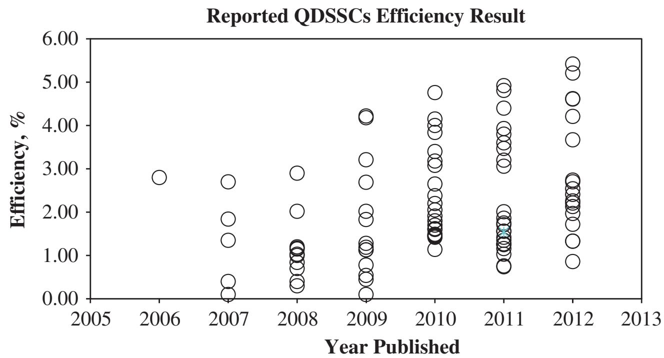


Fig. 9. Summary of the efficiencies of QDSSCs as reported in the literature reviewed that are given in Table 1.

Nano-sulfide/carbon composite counter electrode has also been demonstrated to yield a better performance with highest power conversion efficiency of 3.08% [182]. Better energy conversion efficiency can also be achieved with CoS as counter electrodes as demonstrated by Yang et al. with an efficiency of 3.40% in CdS/CdSe QDSSC utilizing CoS as the CE [183].

In the latest development, composite of reduced graphene oxide (RGO) and Cu_2S as CE has open up another material choice for use in QDSSCs [112,184]. An efficiency as high as 5.42% was reported by Santra et al. in a CdS/CdSe QDSSC with this composite material as the CE [112]. The high performance is also attributed to other factors such as Mn-doped CdS/CdSe QDs and ZnS passivation layer in the QDSSC assembly. Nevertheless, the use Cu_2S/RGO as CE has been verified by Radich et al. [184] who have obtained a better fill factor in a QDSSC. In another development, the use of conducting polymer materials as CEs has shown some promising results due to their low-cost availability, high conductivity, large surface area and good electrocatalytic activity for iodide based electrolytes. Among the candidates, PEDOT has helped to achieve an energy conversion efficiency of 1.35% when used as a CE in a CdS QDSSC [185]. Nevertheless, in depth investigations are in progress to identify other high performing CE materials.

6. Conclusions and perspectives

QDSSCs have become a promising alternative for DSSCs due to the excellent properties of QD sensitizers. Among the wide variety of semiconductor materials available for QDs, Cd chalcogenide has been the preferred choice, especially CdS and CdSe, by many researchers. We have reviewed the research work reported on QDSSCs with the focus on Cd chalcogenide as sensitizers. The fabrication of QDSSCs, their working principle and performance evaluation has also been discussed. The research activities have been focused in improving the overall efficiency of the QDSSC in recent years. In order to achieve improvements and breakthroughs in QDSSCs performance, focus should be channelled to the investigation of materials, surface treatments of photoanode and combined absorbers [186]. Given the limited range of materials that have been investigated so far, researchers have more room to explore and understand the use of new materials in improving the performance of QDSSCs. Based on the works by various researchers, a best performing Cd chalcogenide QDSSC should have high surface area TiO_2 layer as the substrate for maximum attachment of QDs. Ordered network for the main porous substrate for the sensitizers would definitely increase the efficiency of QDSSCs. The sensitized TiO_2 layer should be covered with a passivation layer in order to minimize the electron recombination at the interface of photoanode and electrolyte. An efficient electrolyte and counter electrode (CE) are also important to achieve high fill factors and efficiencies. So far, cobalt based and polysulfide electrolytes have been found to work well in the Cd chalcogenide QDSSCs. Noble materials like Pt and Au are the usual choice for the CE while carbon and composite Cu_2S/RGO are gaining popularity. New materials and improved architecture of solar cell structure could pave way for achieving a high efficiency QDSSC. It is forecasted that the efficiency of QDSSCs could achieve higher value at lower cost should the trend of third generation solar cell as shown in Fig. 1 is materialized. The literature reviewed from recent years augur well with this trend (refer to Table 1 for the summary of the literature reviewed and Fig. 9 shows the summary of the reported efficiencies from the work published from 2006 to 2012). Although the power conversion efficiencies achieved are relatively high in the recent years, the variation in the reported values is mainly due to various methods and parameters used in each research pointing to the possibility of more novel discoveries and innovative research in the near future. Nevertheless, the highest efficiency obtained in each year has been increasing. With this trend, we foresee efficiency above 6% is achievable for Cd chalcogenide QDSSCs in the near future.

Acknowledgments

The authors would like to thank University of Malaya for the IPPP grant no. PV094-2012A. H.K. Jun thanks University of Malaya for the Fellowship Scheme scholarship awarded.

References

[1] Lewis NS, Crabtree G. Basic research needs for solar energy utilization. In: 2005 report on the basic energy sciences workshop on solar energy utilization. U.S. Department of Energy. Available online at: 〈http://www.er.doe.gov/bes/reports/files/SEU_rpt.pdf〉; April 18–21 2005 [accessed August, 2011].
[2] Gratzel M. Dye-sensitized solar cells. Journal of Photochemistry and Photobiology C: Photochemistry 2003;4:145–53.
[3] Blom PWM, Mihailetchi VD, Koster LJA, Markov DE. Device physics of polymer: fullerence bulk heterojunction solar cells. Advanced Materials 2007;19:1551–66.
[4] Peumans P, Uchida S, Forrest SR. Efficient bulk heterjunction photovoltaic cells using small-molecular-weight organic thin films. Nature 2003;425: 158–62.
[5] Kramer IJ, Zhitomirsky D, Bass JD, Rice PM, Topuria T, Krupp L, Thon SM, Ip AH, Debnath R, Kim H-C, Sargent EH. Ordered nanopillar structured electrodes for depleted bulk heterojunction colloidal quantum dot solar cells. Advanced Materials 2012;24:2315–9.
[6] Pattantyus-Abraham AG, Kramer IJ, Barkhouse AR, Wang X, Konstantatos G, Debnath R, Levina L, Raabe I, Nazeeruddin MK, Gratzel M, Sargent EH. Depleted-heterojunction colloidal quantum dot solar cells. ACS Nano 2010;4:3374–80.
[7] Gunes S, Sariciftci NS. Hybrid solar cells. Inorganica Chimica Acta 2008;361:581–8.
[8] McGehee MD. Nanostructured organic-inorganic hybrid solar cells. MRS **Bulletin** 2009;34:95–100.
[9] Chandrasekaran J, Nithyaprakash D, Ajjan KB, Maruthamuthu S, Manoharan D, Kumar S. Hybrid solar cell based on blending of organic and inorganic materials – an overview. Renewable & Sustainable Energy Reviews 2011;15:1228–38.
[10] Werner JH. Second and third generation photovoltaics–dreams and reality. Advances in Solid State Physics 2004;44:51–67.
[11] Shockley W, Queisser HJ. Detailed balance limit of efficiency of p-n junction solar cells. Journal of Applied Physics 1961;32:510–9.
[12] Green MA. Prospect for photovoltaic efficiency enhancement using low-dimensional structures. Nanotechnology 2000;11:401–5.
[13] Green MA. Third generation photovoltaics: advanced solar energy conversion. Berlin, Germany: Springer-Verlag; 2006.
[14] O'Regan B, Gratzel M, Low-cost A. High-efficiency solar cell based on dye-sensitized colloidal TiO_2films. Nature 1991;353:737–40.
[15] Buraidah MH, Teo LP, Yusuf SNF, Noor MM, Kufian MZ, Careem MA, Majid SR, Taha RM, Arof AK. TiO_2/Chitosan-$NH_4I(+I_2)$-BMII-based dye-sensitized solar cells with anthocyanin dyes extracted from black rice and red cabbage. International Journal of Photoenergy 2011;2011 p. 11.

[16] Noor MM, Buraidah MH, Yusuf SNF, Careem MA, Majid SR, Arof AK. Performance of dye-sensitized solar cells with (PVDF-HFP)-KI-EC-PC electrolyte and different dye materials. International Journal of Photoenergy 2011;2011 p. 5.
[17] Kim S, Lee JK, Kang SO, Ko J, Yum J-H, Fantacci S, Angelis FD, Censo DD, Nazeeruddin MK, Gratzel M. Molecular engineering of organic sensitizers for solar cell applications. Journal of the American Chemical Society 2008;128:16701–7.
[18] Vogel R, Pohl K, Weller H. Sensitization of highly porous, polycrystalline TiO_2 electrodes by quantum sized CdS. Chemical Physics Letters 1990;174:241–6.
[19] Vogel R, Hoyer P, Weller H. Quantum-sized PbS, CdS, Ag_2S, Sb_2S_3 and Bi_2S_3 particles as sensitizers for various nanoporous wide-bandgap semiconductors. Journal of Physical Chemistry 1994;98:3183–8.
[20] Kamat PV. Quantum dot solar cells. semiconductor nanocrystals as light harvesters. The Journal of Physical Chemistry C 2008;112:18737–53.
[21] Rühle S, Shalom M, Zaban A. Quantum-dot-sensitized solar cells. ChemPhysChem 2010;11:2290–304.
[22] Yu W, Qu LH, Guo WZ, Peng XG. Experimental determination of the extinction coefficient of CdTe, CdSe, and CdS nanocrystals. Chemistry of Materials 2003;15:2854–60.
[23] Gonzalez-Pedro V, Xu X, Mora-Sero I, Bisquert J. Modeling high-efficiency quantum dot sensitized solar cells. ACS Nano 2010;4:5783–90.
[24] Im J-H, Lee C-R, Lee J-W, Park S-W, Park N-G. 6.5% efficient perovskite quantum-dot-sensitized solar cell. Nanoscale 2011;3:4088–93.
[25] Ip AH, Thon SM, Hoogland S, Voznyy O, Zhitomirsky D, Debnath R, Levina L, Rollny LR, Carey GH, Fischer A, Kemp KW, Kramer IJ, Ning Z, Labelle AJ, Chou KW, Amassian A, Sargent EH. Hybrid passivated colloidal quantum dot solids. Nature Nanotechnology 2012;7:577–82.
[26] Chang J-Y, Su L-F, Li C-H, Chang C-C, Lo J-M. Efficient "green" quantum dot-sensitized solar cells based on Cu_2S–$CuInS_2$–ZnSe architecture. Chemical Communications 2012;48:4848–50.
[27] Peter LM. The Gratzel cell: where next? Journal of Physical Chemistry Letters 2011;2:1861–7.
[28] Gratzel M. Conversion of sunlight to electric power by nanocrystalline dye-sensitized solar cells. Journal of Photochemistry and Photobiology A: Chemistry 2004;164:3–14.
[29] Tennakone K, Kumara GRRA, Kottegoda IRM, Perera VPS. An efficient dye-sensitized photoelectrochemical solar cell made from oxides of tin and zinc. Chemical Communications 1999:15–6.
[30] Sayama K, Sugihara H, Arakawa H. Photoelectrochemical properties of a porous Nb_2O_5electrode sensitized by a ruthenium dye. Chemistry of Materials 1998;10:3825–32.
[31] Nozik AJ. Quantum dot solar cells 2002;E14:115–20Physica 2002;E14: 115–20.
[32] Zaban A, Micic OI, Gregg BA, Nozik AJ. Photosensitization of nanoporous TiO_2 electrodes with InP quantum dots. Langmuir 1998;14:3153–6.
[33] Liu D, Kamat PV. Photoelectrochemical behaviour of thin CdSe and coupled TiO_2/CdSe semiconductor films. Journal of Physical Chemistry 1993;97:10769–73.
[34] Hoyer P, Konenkamp R. Photoconduction in porous TiO_2 Sensitized by PbS quantum dots. Applied Physics Letters 1995;66:349–51.
[35] Yang Z, Chen C-Y, Roy P, Chang H-T. Quantum dot-sensitized solar cells incorporating nanomaterials. Chemical Communications 2011;47:9561–71.
[36] Shalom M, Tachan Z, Bouhadana Y, Barad H-N, Zaban A. Illumination intensity-dependent electronic properties in quantum dot sensitized solar cells. Journal of Physical Chemistry Letters 2011;2:1998–2003.
[37] Robel I, Subramanian V, Kuno M, Kamat PV. Quantum dot solar cells. Harvesting light energy with CdSe nanocrystals molecularly linked to mesoscopic TiO_2 films. Journal of the American Chemical Society 2006;128:2385–93.
[38] Robel I, Kuno M, Kamat PV. Size-dependent electron injection from excited CdSe quantum dots into TiO_2 nanoparticles. Journal of the American Chemical Society 2007;129:4136–7.
[39] Kongkanand A, Tvrdy K, Takechi K, Kuno M, Kamat PV. Quantum dot solar cells. Tuning photoresponse through size and shape control of CdSe-TiO_2architecture. Journal of the American Chemical Society 2008;130: 4007–15.
[40] Chakrapani V, Tvrdy K, Kamat PV. Modulation of electron injection in CdSe–TiO_2 system through medium alkanility. Journal of the American Chemical Society 2010;132:1228–9.
[41] Mora-Sero I, Bisquert J, Dittrich Th, Belaidi A, Susha AS, Rogach AL. Photosensitization of TiO_2 layers with CdSe quantum dots: correlation between light absorption and photoinjection. Journal of Physical Chemistry C 2007;111:14889–92.
[42] Shen Y-J, Lee Y-L. Assembly of CdS quantum dots onto mesoscopic TiO_2 films for quantum dot-sensitized solar cell application. Nanotechnology 2008;19:045602.
[43] Wang X, Koleilat GI, Tang J, Liu H, Kramer IJ, Debnath R, Brzozowski L, Barkhouse DAR, Levina L, Hoogland S, Sargent EH. Tandem colloidal quantum dot solar cells employing a graded recombination layer. Nature Photonics 2011;5:480–4.
[44] Peng ZA, Peng X. Formation of high-quality CdTe, CdSe, and CdS nanocrystals using CdO as precursor. Journal of the American Chemical Society 2001;123:183–4.
[45] Gratzel M. Photoelectrochemical cells. Nature 2001;414:338–44.
[46] Gorer S, Hodes G. Quantum size effects in the study of chemical solution deposition mechanism of semiconductor films. Journal of Physical Chemistry 1994;98:5338–46.
[47] Thambidurai M, Muthukumarasamy N, Agilan S, Murugan N, Vasantha S, Balasundaraprabhu R, Senthil TS. Strong quantum confinement effect in nanocrystalline CdS. Journal of Materials Science 2010;25:3254–8.
[48] Nozik AJ. Exciton multiplication and relaxation dynamics in quantum dots: applications to ultrahigh-efficiency solar photon conversion. Inorganic Chemistry 2005;44:6893–9.
[49] Schaller RD, Klimov VI. High efficiency carrier multiplication in PbSe nanocrystals: implications for solar energy conversion. Physical Review Letters 2004;92:186601.
[50] Ellingson RJ, Beard MC, Johnson JC, Yu P, Micic OI, Nozik AJ, Shabaev A, Efros AL. Highly efficient multiple exciton generation in colloidal PbSe and PbS quantum dots. Nano Letters 2005;5:865–71.
[51] Nozik AZ, Beard MC, Luther JM, Law M, Ellingson RJ, Johnson JC. Semiconductor quantum dots and quantum dot arrays and applications of multiple exciton generation to third-generation photovoltaic solar cells. Chemical Reviews 2010;110:6873–90.
[52] Beard MC. Multiple exciton generation in semiconductor quantum dots. Journal of Physical Chemistry Letters 2011;2:1282–8.
[53] Htoon H, Malko AV, Bussian D, Vela J, Chen Y, Hollingsworth JA, Klimov VI. Highly emissive multiexcitons in steady-state photoluminescence of individual giant CdSe/CdS core/shell nanocrystals. Nano Letters 2010;10:2401–7.
[54] Semonin OE, Luther JM, Choi S, Chen H-Y, Gao J, Nozik AJ, Beard MC. Peak external photocurrent quantum efficiency exceeding 100% via MEG in a quantum dot solar cell. Science 2011;334:1530–3.
[55] Nair G, Bawendi MG. Carrier multiplication yields of CdSe and CdTe nanocrystals by transient photoluminescence spectroscopy. Physical Review B: Condensed Matter and Materials Physics 2007;76:081304.
[56] Scheller RD, Sykora M, Jeong S, Klimov VI. High-efficiency carrier multiplication and ultrafast charge separation in semiconductor nanocrystals studied via time-resolved photoluminescence,. Journal of Physical Chemistry B 2006;110:25332–8.
[57] Califano M. Photoinduced surface trapping and the observed carrier multiplication yields in static CdSe nanocrystal samples. ACS Nano 2011;5: 3614–21.
[58] Hanna MC, Nozik AJ. Solar conversion efficiency of photovoltaic and photoelectrolysis cells with carrier multiplication absorbers. Journal of Applied Physics Letters 2006;100:074510.
[59] Emin S, Singh SP, Han L, Satoh N, Islam A. Colloidal quantum dot solar cells. Solar Energy 2011;85:1264–82.
[60] Chen H, Li W, Liu H, Zhu L. A suitable deposition method of CdS for high performance CdS-sensitized ZnO electrodes: Sequential chemical bath deposition. Solar Energy 2010;84:1201–7.
[61] Zhu G, Pan L, Xu T, Sun Z. Microwave assisted chemical bath deposition of CdS on TiO_2 film for quantum dot-sensitized solar cells,. Journal of Electroanalytical Chemistry 2011;659:205–8.
[62] Zhu G, Pan L, Xu T, Sun Z. CdS/CdSe-cosensitized TiO2 photoanode for quantum-dot-sensitized solar cells by a microwave-assisted chemical bath deposition method. ACS Applied Materials & Interfaces 2011;3:3146–51.
[63] Senthamilselvi V, Saravanakumar K, Begum NJ, Anandhi R, Ravichandran AT, Sakthivel B, Ravichandran K. Photovoltaic properties of nanocrystalline CdS films deposited by SILAR and CBD techniques—a comparative study. Journal of Materials Science: Materials in Electronics 2012;23:302–8.
[64] Toyoda T, Sato J, Shen Q. Effect of sensitization by quantum-sized CdS on photoacoustic and photoelectrochemical current spectra of porous TiO_2 electrodes. Review of Scientific Instruments 2003;74:297–9.
[65] Lee HJ, Wang M, Chen P, Gamelin DR, Zakeeruddin SM, Gratzel M, Nazeeruddin MK. Efficient CdSe quantum dot-sensitized solar cells prepared by an improved successive ionic layer adsorption and reaction process. Nano Letters 2009;9:4221–7.
[66] Barcelo I, Lana-Villarreal T, Gómez R. Efficient sensitization of ZnO nanoporous films with CdSe QDs grown by successive ionic layer adsorption and reaction (SILAR). Journal of Photochemistry and Photobiology A: Chemistry 2011;220:47–53.
[67] Qian S, Wang C, Lu W, Zhu Y, Yao W, Lu X. An enhanced CdS/TiO_2 photocatalyst with high stability and activity: effect of mesoporous substrate and bifunctional linking molecule. Journal of Materials Chemistry 2011;21:4945–52.
[68] Murray CB, Norris DJ, Bawendi MG. Synthesis and characterization of nearly monodisperse CdE (E=S, Se, and Te) semiconductor nanocrystallites. Journal of the American Chemical Society 1993;115:8706–15.
[69] Gimenez S, Mora-Sero I, Macor L, Guijarro N, Lana-Villarreal T, Gómez R, Diguna LJ, Shen Q, Toyoda T, Bisquert J. Improving the performance of colloidal quantum-dot-sensitized solar cells. Nanotechnology 2009;20: 295204.
[70] Guijarro N, Lana-Villarreal T, Mora-Sero I, Bisquert J, Gómez R. CdSe quantum dot-sensitized TiO_2 electrodes: effect of quantum dot coverage and mode of attachment. Journal of Physical Chemistry C 2009;113:4208–14.
[71] Wijayantha KGU, Peter LM, Otley LC. Fabrication of CdS quantum dot sensitized solar cells via a pressing route. Solar Energy Materials and Solar Cells 2004;83:363–9.
[72] Salant A, Shalom M, Hod I, Faust A, Zaban A, Banin U. Quantum dot sensitized solar cells with improved efficiency prepared using electrophoretic deposition. ACS Nano 2010;4:5962–8.

[73] Poulose AC, Veeranarayanan S, Varghese SH, Yoshida Y, Maekawa T, Kumar DS. Functionalized electrophoretic deposition of CdSe quantum dots onto TiO_2 electrode for photovoltaic application. Chemical Physics Letters 2012;539–540:197–203.
[74] Lee YH, Im SY, Lee J-H, Seok SI. Porous CdS-sensitized electrochemical solar cells. Electrochimica Acta 2011;56:2087–91.
[75] Zhu G, Lv T, Pan L, Sun Z, Sun C. All spray pyrolysis deposited CdS sensitized ZnO films for quantum dot-sensitized solar cells. Journal of Alloys and Compounds 2011;509:362–5.
[76] Kashyout AB, Soliman HMA, Fathy M, Gomaa EA, Zidan AA. CdSe quantum dots for solar cell devices. International Journal of Photoenergy 2012;2012 p. 7.
[77] Zhu L, An W-J, Springer JW, Modesto-Lopez LB, Gullapalli S, Holten D, Wong MS, Biswas P. Linker-free quantum dot sensitized TiO_2 photoelectrochemical cells. International Journal of Hydrogen Energy 2012;37:6422–30.
[78] Joo J, Kim D, Yun D-J, Jun H, Rhee S-W, Lee JS, Yong K, Kim S, Jeon S. The fabrication of highly uniform ZnO/CdS core/shell structures using a spin-coating-based successive ion layer adsorption and reaction method. Nanotechnology 2010;21:325604.
[79] Feng J, Han J, Zhao X. Synthesis of $CuInS_2$ quantum dots on TiO_2 porous films by solvothermal method for absorption layer of solar cells. Progress in Organic Coating 2009;64:268–73.
[80] Plass R, Pelet S, Krueger J, Gratzel M, Bach,Quantum U. dot sensitization of organic-inorganic hybrid solar cells. Journal of Physical Chemistry B 2002;106:7578–80.
[81] Yu P, Zhu K, Norman AG, Ferrere S, Frank AJ, Nozik AJ. Nanocrystalline TiO_2 solar cells sensitized with InAs quantum dots. Journal of Physical Chemistry 2006;B110:25451–4.
[82] Tubtimtae A, Wu K-L, Tung H-Y, Lee M-W, Wang GJ. Ag_2S quantum dot-sensitized solar cells. Electrochemistry Communications 2010;12:1158–60.
[83] Xie Y, Yoo SH, Chen C, Cho SO. Ag_2S quantum dots-sensitized TiO_2 nanotube array photoelectrodes. Materials Science and Engineering B 2012;177: 106–11.
[84] Lee HJ, Kim D-Y, Yoo J-S, Bang J, Kim S, Park S-M. Anchoring cadmium chalcogenide quantum dots (QD) onto stable oxide semiconductor for QD sensitized solar cells. Bulletin of the Korean Chemical Society 2007;28: 953–8.
[85] Ning Z, Tian H, Yuan C, Fu Y, Qin H, Sun L, Agren H. Solar cells sensitized with type-II ZnSe–CdS core/shell colloidal quantum dots. Chemical Communications 2011;47:1536–8.
[86] Kontos AG, Likodimos V, Vassalou E, Kapogianni I, Raptis YS, Raptis C, Falaras P. Nanostructured titania films sensitized by quantum dot chalcogenides. Nanoscale Research Letters 2011;6:266–71.
[87] Hossain MF, Biswas S, Zhang ZH, Takahashi T. Bubble-like CdSe nanoclusters sensitized TiO_2 nanotube arrays for improvement in solar cell. Photochemistry and Photobiology A: Chemistry 2011;217:68–75.
[88] Chen J, Lei W, Deng WQ. Reduced charge recombination in a co-sensitized quantum dot solar cell with two different sizes of CdSe quantum dot. Nanoscale 2011;3:674–7.
[89] Sung TK, Kang JH, Jang DM, Myung Y, Jung GB, Kim HS, Jung CS, Cho YJ, Park J, Lee C-L. CdSSe layer-sensitized TiO_2 nanowire arrays as efficient photoelectrodes. Journal of Materials Chemistry 2011;21:4553–61.
[90] Li JJ, Wang YA, Guo WZ, Keay JC, Mishima TD, Johnson MB, Peng XG. Large-scale synthesis of nearly monodisperse CdSe/CdS Core/shell nanocrystals using air-stable reagents via successive ion layer adsorption and reaction. Journal of the American Chemical Society 2003;125:12567–75.
[91] Bridge CJ, Dawson P, Buckle PD, Ozsan ME. Low temperature photoluminescence spectroscopy of thin film, polycrystalline CdTe/ CdS solar cell structures. Semiconductor Science and Technology 2000;15:975–9.
[92] Luan C, Vaneski A, Susha AS, Xu X, Wang H-E, Chen X, Xu J, Zhang W, Lee C-S, Rogach AL, Zapien JA. Facile solution growth of vertically aligned ZnO nanorods sensitized with aqueous CdS and CdSe quantum dots for photovoltaic applications. Nanoscale Research Letters 2011;6:340–7.
[93] Lee Y-L, Lo Y-S. Highly efficient quantum-dot-sensitized solar cell based on co-sensitization of CdS/CdSe. Advanced Functional Materials 2009;9:604–9.
[94] Dworak L, Matylitsky VV, Breus VV, Braun M, Basche T, Wachtveitl J. Ultrafast charge separation at the CdSe/CdS core/shell quantum dot/ methylviologen interface: Implications for nanocrystal solar cells. Journal of Physical Chemistry C 2011;115:3949–55.
[95] Shalom M, Dor S, Ruhle S, Grinis L, Zaban A. Core/CdS quantum dot/shell mesoporous solar cells with improved stability and efficiency using an amorphous TiO_2 coating. Journal of Physical Chemistry C 2009;113:3895–8.
[96] Braga A, Gimenez S, Concina I, Vomiero A, Mora-Sero I. Panchromatic sensitized solar cells based on metal sulfide quantum dots grown directly on nanostructured TiO_2 electrodes. Journal of Physical Chemistry Letters 2011;2:454–60.
[97] Li T-L, Lee Y-L, Teng H. $CuInS_2$ quantum dots coated with CdS as high-performance sensitizers for TiO_2 electrodes in photoelectrochemical cells. Journal of Materials Chemistry 2011;21:5089–98.
[98] Lee HJ, Bang J, Park J, Kim S, Park S-M. Multilayered semiconductor (CdS/CdSe/ZnS)-sensitized TiO_2 mesoporous solar cells: all prepared by successive ionic layer adsorption and reaction processes. Chemistry of Materials 2010;22:5636–43.
[99] Cheng S, Fu W, Yang H, Zhang L, Ma J, Zhao H, Sun M, Yang L. Photoelectrochemical performance of multiple semiconductors (CdS/CdSe/ZnS) cosensitized TiO_2 photoelectrodes. Journal of Physical Chemistry C 2012;116:2615–21.
[100] Mora-Sero I, Dittrich T, Susha AS, Rogach AL, Bisquert J. Large improvement of electron extraction from CdSe quantum dots into a TiO_2 thin layer by N3 dye coabsorption. Thin Solid Films 2008;516:6994–8.
[101] Song X, Yu X-L, Xie Y, Sun J, Ling T, Du X-W. Improving charge separation of solar cells by the co-sensitization of CdS quantum dots and dye. Semiconductor Science and Technology 2010;25:095014.
[102] Fan S-Q, Cao R-J, Xi Y-X, Gao M, Wang M-D, Kim D-H, Kim C-W, Ko J-J. CdSe quantum dots as co-sensitizers of organic dyes in solar cells for red-shifted light harvesting. Journal of Optoelectronics and Advanced Materials 2009;3:1027–33.
[103] Lee HJ, Leventis HC, Moon S-J, Chen P, Ito S, Haque SA, Torres T, Nuesch F, Geiger T, Zakeeruddin SM, Gratzel M, Nazeeruddin MJ. PbS and CdS quantum dot-sensitized solid-state solar cells: “Old concepts, new results”. Advanced Functional Materials 2009;19:2735–42.
[104] Choi H, Nicolaescu R, Paek S, Ko J, Kamat PV. Supersensitization of CdS quantum dots with a near-infrared organic dye: toward the design of panchromatic hybrid-sensitized solar cells. ACS Nano 2011;5:9238–45.
[105] Buhbut S, Itzhakov S, Tauber E, Shalom M, Hod I, Geiger T, Garini Y, Oron D, Zaban A. Built-in quantum dot antennas in dye-sensitized solar cells. ACS Nano 2010;4:1293–8.
[106] Lee HJ, Chang DW, Park S-M, Zakeeruddin SM, Gratzel M, Nazeeruddin MK. CdSe quantum dot (QD) and molecular dye-hybrid sensitizers for TiO_2 mesoporous solar cells: working together with a common hole carrier of cobalt complexes. Chemical Communications 2010;46:8788–90.
[107] So S, Fan S-Q, Choi H, Kim C, Cho N, Song K, Ko J. Stepwise cosensitization through chemically bonding organic dye to CdS quantum-dot-sensitized TiO_2 electrode. Applied Physics Letters 2010;97:263506.
[108] Ling T, Wu M-K, Niu K-Y, Yang J, Gao Z-M, Sun J, Du X-W. Spongy structure of CdS nanocrystals decorated with dye molecules for semiconductor sensitized solar cells. Journal of Materials Chemistry 2011;21:2883–9.
[109] Shalom M, Albero J, Tachan Z, Martinez-Ferrero E, Zaban A, Palomares E. Quantum dot-dye bilayer-sensitized solar cells: breaking the limits imposed by the low absorbance of dye monolayers. Journal of Physical Chemistry Letters 2010;1:1134–8.
[110] Mora-Sero I, Gimenez S, Moehl T, Fabregat-Santiago F, Lana-Villareal T, Gómez R, Bisquert J. Factors determining the photovoltaic performance of a CdSe quantum dot sensitized solar cell: the role of the linker molecule and of the counter electrode. Nanotechnology 2008;19:424007.
[111] Chen J, Zhao DW, Song JL, Sun XW, Deng WQ, Liu XW, Lei W. Directly assembled CdSe quantum dots on TiO_2 in aqueous solution by adjusting pH value for quantum dot sensitized solar cells. Electrochemistry Communications 2009;11:2265–7.
[112] Santra PK, Kamat PV. Mn-doped quantum dot sensitized solar cells: a strategy to boost efficiency over 5%. Journal of the American Chemical Society 2012;134:2508–11.
[113] Hod I, Gonzalez-Pedro V, Tachan Z, Fabregat-Santiago F, Mora-Sero I, Bisquert J, Zaban A. Dye versus quantum dots in sensitized solar cells: participation of quantum dot absorber in the recombination process. Journal of Physical Chemistry Letters 2011;2:3032–5.
[114] Gimenez S, Lana-Villareal T, Gómez R, Agouram S, Munoz-Sanjose V, Mora-Sero I. Determination of limiting factors of photovoltaic efficiency in quantum dot sensitized solar cells: correlation between cell performance and structural properties. Journal of Applied Physics 2010;108:064310.
[115] Martinez-Ferrero E, Sero IM, Albero J, Gimenez S, Bisquert J, Palomares E. Charge transfer kinetics in CdSe quantum dot sensitized solar cells. Physical Chemistry Chemical Physics 2010;12:2819–21.
[116] Guijarro N, Lana-Villarreal T, Shen Q, Toyoda T, Gomez R. Sensitization of titanium dioxide photoanodes with cadmium selenide quantum dots prepared by SILAR: photoelectrochemical and carrier dynamics studies. Journal of Physical Chemistry C 2010;114:21928–37.
[117] Pernik DR, Tvrdy K, Radich JG, Kamat PV. Tracking the adsorption and electron injection rates of CdSe quantum dots on TiO_2: linked versus direct attachment. Journal of Physical Chemistry C 2011;115:13511–9.
[118] Xu X, Gimenez S, Mora-Sero I, Abate A, Bisquert J, Xu G. Influence of cysteine adsorption on the performance of CdSe quantum dots sensitized solar cells. Materials Chemistry and Physics 2010;124:709–12.
[119] Samadpour M, Gimenez S, Boix PP, Shen Q, Calvo ME, Taghavinia N, Irajizad A, Toyoda T, Miguez H, Mora-Sero I. Effect of nanostructured electrode architecture and semiconductor deposition strategy on the photovoltaic performance of quantum dot sensitized solar cells. Electrochimica Acta 2012;75:139–47.
[120] Ruhle S, Yahav S, Greenwald S, Zaban A. The importance of recombination at the TCO/electrolyte interface for high efficiency quantum dot sensitized solar cells. Journal of Physical Chemistry C 2012;116:17473–8.
[121] Tachibana Y, Umekita K, Otsuka Y, Kuwabata S. Performance improvement of CdS quantum dots sensitized TiO_2 solar cells by introducing a dense TiO_2 blocking layer. Journal of Physics D: Applied Physics 2008;41:102002.
[122] Diguna LJ, Shen Q, Kobayashi J, Toyoda T. High efficiency of CdSe quantum-dot-sensitized TiO_2inverse opal solar cells. Applied Physics Letters 2007;91:023116.
[123] Lee Y-L, Huang B-M, Chien H-T. Highly efficient CdSe-sensitized TiO_2 photoelectrode for quantum-dot-sensitized solar cell applications. Chemistry of Materials 2008;20 6903–6095.
[124] Shen Q, Kobayashi J, Diguna LJ, Toyoda T. Effect of ZnS coating on the photovoltaic properties of CdSe quantum dot-sensitized solar cells. Journal of Applied Physics 2008;103:084304.

[125] Guijarro N, Campina JM, Shen Q, Toyoda T, Lana-Villarreal T, Gomez R. Uncovering the role of the ZnS treatment in the performance of quantum dot sensitized solar cells. Physical Chemistry Chemical Physics 2011;13:12024–32.

[126] Liu Z, Miyauchi M, Uemura Y, Cui Y, Hara K, Zhao Z, Sunahara K, Furube A. Enhancing the performance of quantum dots sensitized solar cell by SiO_2 surface coating. Applied Physics Letters 2010;96:233107.

[127] Samadpour M, Boix PP, Gimenez S, Zad AI, Taghavinia N, Mora-Sero I, Bisquert J. Fluorine treatment of TiO_2 for enhancing quantum dot sensitized solar cell performance. Journal of Physical Chemistry 2011;C115:14400–7.

[128] Tena-Zaera R, Katty A, Bastide S, Levy-Clement C. Annealing effects on the physical properties of electrodeposited ZnO/CdSe core–shell nanowire arrays. Chemistry of Materials 2007;19:1626–32.

[129] Yu X-Y, Lei B-X, Kuang D-B, Su C-Y. High performance and reduced charge recombination of CdSe/CdS quantum dot-sensitized solar cells. Journal of Materials Chemistry 2012;22:12058–63.

[130] Farrow B, Kamat PV. CdSe quantum dot sensitized solar cells. Shuttling electrons through stacked carbon nanocups. Journal of the American Chemical Society 2009;131:11124–31.

[131] Senthil TS, Muthukumarasamy N, Thambidurai M, Balasundaraprabhu R, Agilan,Light S. conversion efficiency of flower like structure TiO_2 thin film solar cells. Journal of Sol–Gel Science and Technology 2011;58:296–301.

[132] Chen H, Fu W, Yang H, Sun P, Zhang Y, Wang L, Zhao W, Zhou X, Zhao H, Jing Q, Qi X, Li Y. Photosensitization of TiO_2 nanorods with CdS quantum dots for photovoltaic devices. Electrochimica Acta 2010;56:919–24.

[133] Gao X-F, Sun W-T, Ai G, Peng L-M. Photoelectric performance of TiO_2 nanotube array photoelectrodes cosensitized with CdS/CdSe quantum dots. Applied Physics Letters 2010;96:153104.

[134] Wang H, Bai Y, Zhang H, Zhang Z, Li J, Guo L. CdS quantum dots-sensitized TiO_2 nanorod array on transparent conductive glass photoelectrodes. Journal of Physical Chemistry C 2010;114:16451–5.

[135] Zeng T, Tao H, Sui X, Zhou X, Zhao X. Growth of free-standing TiO_2 nanorod arrays and its application in CdS quantum dots-sensitized solar cells. Chemical Physics Letters 2011;508:130–3.

[136] Wang C, Jiang Z, Wei L, Chen Y, Jiao J, Eastman M, Liu H. Photosensitization of TiO_2 nanorods with CdS quantum dots for photovoltaic applications: a wet-chemical approach. Nano Energy 2012;1:440–7.

[137] Kang SH, Lee W, Kim HS. Effect of CdS sensitization on single crystalline TiO_2 nanorods in photoelectrochemical cells. Materials Letters 2012;85:74–6.

[138] Xia M, Wang F, Wang Y, Pan A, Zou B, Zhang Q, Wang Y. TiO_2 nanowires sensitized with CdS quantum dots and the surface photovoltage properties. Material Letters 2010;64:1688–90.

[139] Yu K, Chen J. Enhancing solar cell efficiencies through 1D nanostructures. Nanoscale Research Letters 2009;4:1–10.

[140] Chen J, Li C, Zhao DW, Lei W, Zhang Y, Cole MT, Chu DP, Wang BP, Cui YP, Sun XW, Milne WI. A quantum dot sensitized solar cell based on vertically aligned carbon nanotube templated ZnO arrays. Electrochemistry Communications 2010;12:1432–5.

[141] Chen H, Zhu L, Li W, Liu H. Synthesis and photoelectrochemical behavior of CdS quantum dots-sensitized indium-tin-oxide mesoporous film. Current Applied Physics 2012;12:129–33.

[142] Li Y, Pang A, Zheng X, Wei M. CdS quantum-dot-sensitized Zn_2SnO_4 solar cell. Electrochimica Acta 2011;56:4902–6.

[143] Liu L, Hensel J, Fitzmorris RC, Li Y, Zhang JZ. Preparation and photoelectrochemical properties of CdSe/TiO_2 hybrid mesoporous structures. Journal of Physical Chemistry Letters 2010;1:155–60.

[144] Zhu G, Cheng Z, Lv T, Pan L, Zhao Q, Sun Z. Zn-doped nanocrystalline TiO_2 films for CdS quantum dot sensitized solar cells. Nanoscale 2010;2:1229–32.

[145] Zhu G, Su F, Lv T, Pan L, Sun Z. Au nanoparticles as interfacial layer for CdS quantum dot-sensitized solar cells. Nanoscale Research Letters 2010;5: 1749–54.

[146] Zhu G, Xu T, Lv T, Pan L, Zhao Q, Sun Z. Graphene-incorporated nanocrystalline TiO_2 films for CdS quantum dot-sensitized solar cells. Journal of Electroanalytical Chemistry 2010;650:248–51.

[147] Jung M-H, Kang MG. Enhanced photo-conversion efficiency of CdSe–ZnS core-shell quantum dots with Au nanoparticles on TiO_2 electrodes. Journal of Materials Chemistry 2011;21:2694–700.

[148] Lightcap IV, Kamat PV. Fortification of CdSe quantum dots with graphene oxide. Excited state interactions and light energy conversion. Journal of the American Chemical Society 2012;134:7109–16.

[149] Liu L, Wang G, Li Y, Li Y, Zhang JZ. CdSe quantum dot-sensitized Au/TiO_2 hybrid mesoporous films and their enhanced photoelectrochemical performance. Nano Research 2011;4:249–58.

[150] Lopez-Luke T, Wolcott A, Xu L-P, Chen S, Wen Z, Li J, Rosa EDL, Zhang JZ. Nitrogen-doped and CdSe quantum-dot-sensitized nanocrystalline TiO_2 films for solar energy conversion applications. Journal of Physical Chemistry C 2008;112:1282–92.

[151] Shu T, Xiang P, Zhou Z-M, Wang H, Liu G-H, Han H-W, Zhao Y-D. Mesoscopic nitrogen-doped TiO_2 spheres for quantum dot-sensitized solar cells. Electrochimica Acta 2012;68:166–71.

[152] Zhu G, Pan L, Xu T, Zhao Q, Sun Z. Cascade structure of TiO_2/ZnO/CdS film for quantum dot sensitized solar cells. Journal of Alloys and Compounds 2011;509:7814–8.

[153] Zhang Q, Guo X, Huang X, Huang S, Li D, Luo Y, Shen Q, Toyoda T, Meng Q. Highly efficient CdS/CdSe-sensitized solar cells controlled by the structural properties of compact porous TiO_2 photoelectrodes. Physical Chemistry Chemical Physics 2011;13:4659–67.

[154] Tian J, Gao R, Zhang Q, Zhang S, Li Y, Lan J, Qu X, Cao G. Enhanced performance of CdS/CdSe quantum dot cosensitized solar cells via homogeneous distribution of quantum dots in TiO_2 film. Journal of Physical Chemistry 2012;116:18655–62.

[155] Hossain MA, Jennings JR, Shen C, Pan JH, Koh ZY, Mathews N, Wang Q. CdSe-sensitized mesoscopic TiO_2 solar cells exhibiting $>5\%$ efficiency: redundancy of CdS buffer layer. Journal of Materials Chemistry 2012;22:16235–42.

[156] Zhang Q, Chen G, Yang Y, Shen X, Zhang Y, Li C, Yu R, Luo Y, Li D, Meng Q. Toward highly efficient CdS/CdSe quantum dots-sensitized solar cells incorporating ordered photoanodes on transparent conductive substrates. Physical Chemistry Chemical Physics 2012;14:6479–86.

[157] Zhao F, Tang G, Zhang J, Lin Y. Improved performance of CdSe quantum dot-sensitized TiO_2 thin film by surface treatment with $TiCl_4$. Electrochimica Acta 2012;62:396–401.

[158] Kim J, Choi H, Nahm C, Kim C, Nam S, Kang S, Jung D-R, Kim JI, Kang J, Park B. The role of a $TiCl_4$ treatment on the performance of CdS quantum-dot-sensitized solar cells. Journal of Power Sources 2012;220:108–13.

[159] Liu Z, Li Y, Zhao Z, Cui Y, Hara K, Miyauchi M. Block copolymer templated nanoporous TiO_2 for quantum-dot-sensitized solar cells. Journal of Materials Chemistry 2010;20:492–7.

[160] Lai C-H, Chou P-T. All chemically deposited, annealing and mesoporous metal oxide free CdSe solar cells. Chemical Communications 2011;47:3448–50.

[161] Patil SB, Singh AK. Electrodeposited vertically aligned ZnO nanorods thin films on steel substrate for CdS quantum dots sensitized solar cell. Electrochimica Acta 2011;56:5693–701.

[162] Ogermann D, Wilke T, Kleinermanns K. CdS_xSe_y/TiO_2 solar cell prepared with sintered mixture deposition. Open Journal of Physical Chemistry 2012;2:47–57.

[163] Samadpour M, Irajizad A, Taghavinia N, Molaei M. A new structure to increase the photostability of CdTe quantum dot sensitized solar cells. Journal of Physics D: Applied Physics 2011;44:045103.

[164] Lee HJ, Yum J-H, Leventis HC, Zakeeruddin SM, Haque SA, Chen P, Seok SI, Gratzel M, Nazeeruddin MK. CdSe quantum dot-sensitized solar cells exceeding efficiency 1% at full sun intensity. Journal of Physical Chemistry 2008;C112:11600–8.

[165] Lee HJ, Chen P, Moon S-J, Frederic S, Sivula K, Bessho T, Gamelin DR, Comte P, Zakeeruddin SM, Seok SI, Gratzel M, Nazeeruddin MK. Regenerative PbS and CdS quantum dot sensitized solar cells with a cobalt complex as hole mediator. Langmuir 2009;25:7602–8.

[166] Lee Y-L, Chang C-H. Efficient polysulfide electrolyte for CdS quantum dot-sensitized solar cells. Journal of Power Sources 2008;185:584–8.

[167] Bang JH, Kamat PV. Quantum dot sensitized solar cells: a tale of two semiconductor nanocrystal: CdSe and CdTe. ACS Nano 2009;3:1467–76.

[168] Chakrapani V, Baker D, Kamat PV. Understanding the role of the sulfide redox couple (S^{2-}/S_n^{2-}) in quantum dot-sensitized solar cells. Journal of the American Chemical Society 2011;133:9607–15.

[169] Chou C-Y, Lee C-P, Vittal R, Ho K-C. Efficient quantum dot-sensitized solar cell with polystyrene-modified TiO_2 photoanode and with guanidine thiocyanate in its polysulfide electrolyte. Journal of Power Sources 2011;19:6595–602.

[170] Jovanovski V, Gonzalez-Pedro V, Gimenez S, Azaceta E, Cabanero G, Grande H, Tena-Zaera R, Mora-Sero I, Bisquert J. A sulfide/polysulfide-based ionic liquid electrolyte for quantum dot-sensitized solar cells. Journal of the American Chemical Society 2011;133:20156–9.

[171] Fuke N, Hoch LB, Koposov AY, Manner VW, Werder DJ, Fukui A, Koide N, Katayama H, Sykora M. CdSe quantum-dot-sensitized solar cell with $\sim$100% internal quantum efficiency. ACS Nano 2010;4:6377–86.

[172] Qian J, Liu Q-S, Li G, Jiang K-J, Yang L-M, Song Y. P3HT as hole transport material and assistant light absorber in CdS quantum dots-sensitized solid-state solar cells. Chemical Communications 2011;47:6461–3.

[173] Yu Z, Zhang Q, Qin D, Luo Y, Li D, Shen Q, Toyoda T, Meng Q. Highly efficient quasi-solid-state quantum-dot-sensitized solar cell based on hydrogel electrolytes. Electrochemistry Communications 2010;12:1776–9.

[174] Zhang Q, Zhang Y, Huang S, Huang X, Luo Y, Meng Q, Li D. Application of carbon counterelectrode on CdS quantum dot-sensitized solar cells (QDSSCs). Electrochemistry Communications 2010;12:327–30.

[175] Fang B, Kim M, Fan S-Q, Kim JH, Wilkinson DP, Ko J, Yu J-S. Facile synthesis of open mesoporous carbon nanofibers with tailored nanostructure as a highly efficient counter electrode in CdSe quantum-dot-sensitized solar cells. Journal of Materials Chemistry 2011;21:8742–8.

[176] Sudhagar P, Ramasamy E, Cho W-H, Lee J, Kang YS. Robust mesocellular carbon foam counter electrode for quantum-dot sensitized solar cells. Electrochemistry Communications 2011;13:34–7.

[177] Huang X, Huang S, Zhang Q, Guo X, Li D, Luo Y, Shen Q, Toyoda T, Meng Q. A flexible photoelectrode for CdS/CdSe quantum-dot-sensitized solar cells (QDSCCs). Chemical Communications 2011;47:2664–6.

[178] Chong L-W, Chien H-T, Lee Y-L. Assembly of CdSe onto mesoporous TiO_2 films induced by self-assembled monolayer of quantum dot-sensitized solar cell applications. Journal of Power Sources 2010;195:5109–13.

[179] Seol M, Kim H, Tak Y, Yong K. Novel nanowire array based highly efficient quantum dot sensitized solar cell. Chemical Communications 2010;46:5521–3.

[180] Yu X-Y, Lei B-X, Kuang D-B, Su C-Y. Highly efficient CdTe/CdS quantum dot sensitized solar cells fabricated by a one-step linker assisted chemical bath deposition. Chemical Science 2011;2:1396–400.

[181] Zewdu T, Clifford JN, Hernandez JP, Palomares E. Photo-induced charge transfer dynamics TiO2/CdS/CdSe sensitized solar cells. Energy Environmental Science 2011;4:4633–8.

[182] Deng M, Zhang Q, Huang S, Li D, Luo Y, Shen Q, Toyoda T, Meng Q. Low-cost flexible nano-sulfide/carbon composite counter electrode for quantum-dot-sensitized solar cell. Nanoscale Research Letters 2010;5:986–90.
[183] Yang Z, Chen C-Y, Liu C-W, Chang H-T. Electrocatalytic sulphur electrodes for CdS/CdSe quantum dot-sensitized solar cells. Chemical Communications 2010;46:5485–7.
[184] Radich JG, Dwyer R, Kamat PV. Cu_2S reduced graphene oxide composite for high-efficiency quantum dot solar cells. Overcoming the redox limitations of S_2^-/S_n^{2-} at the counter electrode. Journal of Physical Chemistry Letters 2011;2:2453–60.
[185] Yeh M-H, Lee C-P, Chou C-Y, Lin L-Y, Wei H-Y, Chu C-W, Vittal R, Ho K-C. Conducting polymer-based counter electrode for quantum-dot-sensitized solar cell (QDSSC) with a polysulfide electrolyte. Electrochimica Acta 2011;57:277–84.
[186] Mora-Sero I, Bisquert J. Breakthroughs in the development of semiconductor-sensitized solar cells. Journal of Physical Chemistry Letters 2010;1:3046–52.
[187] Fang J, Wu J, Lu X, Shen Y, Lu Z. Sensitization of nanocrystalline TiO_2 electrode with quantum sized CdSe and ZnTcPc molecules. Chemical Physics Letters 1997;270:145–51.
[188] Peter LM, Riley DJ, Tull EZ, Wijayantha KGU. Photosensitization of nanocrystalline TiO_2 by self-assembled layers of CdS quantum dots. Chemical Communications 2002:1030–1.
[189] Shen Q, Arae D, Toyoda T. Photosensitization of nanostructured TiO_2 with CdSe quantum dots: effects of microstructure and electron transport in TiO_2 substrates. Journal of Photochemistry and Photobiology A: Chemistry 2004;164:75–80.
[190] Toyoda T, Tsuboya I, Chen Q. Effect of rutile-type content on nanostructured anatase-type TiO_2 electrode sensitized with CdSe quantum dots characterized with photoacoustic and photoelectrochemical current spectroscopies. Materials Science Engineering C 2005;25:853–7.
[191] Niitsoo O, Sarkar SK, Pejoux C, Ruhle S, Cahen D, Hodes G. Chemical bath deposited CdS/CdSe-sensitized porous TiO_2 solar cells. Journal of Photochemistry and Photobiology A: Chemistry 2006;181:306–13.
[192] Shen Q, Sato T, Hashimoto M, Chen C, Toyoda T. Photoacoustic and photoelectrochemical characterization of CdSe-sensitized TiO_2 electrodes composed of nanotubes and nanowires. Thin Solid Films 2006;499:299–305.
[193] Chang C-H, Lee Y-L. Chemical bath deposition of CdS quantum dots onto mesoscopic TiO_2 films for application in quantum-dots-sensitized solar cells. Applied Physics Letters 2007;91:053503.
[194] Leschkies KS, Divakar R, Basu J, Enache-Pommer E, Boercker JE, Carter CB, Kortshagen UR, Norris DJ, Aydil ES. Photosensitization of ZnO nanowires with CdSe quantum dots for photovoltaic devices. Nano Letters 2007;7:1793–8.
[195] Lin S-C, Lee Y-L, Chang C-H, Shen Y-J, Yang Y-M. Quantum-dot-sensitized solar cells: assembly of CdS-quantum-dots coupling techniques of self-assembled monolayer and chemical bath deposition. Applied Physics Letters 2007;90:143517.
[196] Shen Q, Yanai M, Katayama K, Sawada T, Toyoda T. Optical absorption, photosensitzation, and ultrafast carrier dynamic investigations of CdSe quantum dots grafted onto nanostructured SnO_2 electrode and fluorine-doped tin oxide (FTO) glass. Chemical Physics Letters 2007;442:89–96.
[197] Lee W, Kwak W-C, Min SK, Lee J-C, Chae W-S, Sung Y-M, Han S-H. Spectral broadening in quantum dots-sensitized photoelectrochemical solar cells based on CdSe and Mg-doped CdSe nanocrystals. Electrochemistry Communications 2008;10:1699–702.
[198] Lee WJ, Kang SH, Min SK, Sung Y-E, Han S-H. Co-sensitization of vertically aligned TiO_2 nanotubes with two different sizes of CdSe quantum dots for broad spectrum. Electrochemistry Communications 2008;10:1579–82.
[199] Chen J, Li C, Song JL, Sun XW, Lei W, Deng WQ. Bilayer ZnO nanostructure fabricated by chemical bath and its application in quantum dot sensitized solar cell. Applied Surface Science 2009;255:7508–11.
[200] Chen J, Song JL, Sun XW, Deng WQ, Jiang CY, Lei W, Huang JH, Liu RS. An olei acid-capped CdSe quantum-dot sensitized solar cell. Applied Physics Letters 2009;94:153115.
[201] Fan S-Q, Kim D, Kim J-J, Jung DW, Kang SO, Ko J. Highly efficient CdSe quantum-dot-sensitized TiO_2 photoelectrodes for solar cell application. Electrochemistry Communications 2009;11:1337–9.
[202] Gao XF, Li HB, Sun WT, Chen Q, Tang FQ, Peng LM. CdTe quantum dots-sensitized TiO_2 nanotube array photoelectrodes. Journal of Physical Chemistry 2009;C113:7531–5.
[203] Hossain MF, Biswas S, Takahashi T. Study of CdS-sensitized solar cells, prepared by ammonia-free chemical bath technique. Thin Solid Films 2009;518:1599–602.
[204] Lan G-Y, Yang Z, Lin Y-W, Lin Z-H, Liao H-Y, Chang H-T. A simple strategy for improving the energy conversion of multilayered CdTe quantum dot-sensitized solar cells. Journal of Materials Chemistry 2009;19:2349–55.
[205] Lee W, Min SK, Dhas V, Ogale SB, Han S-H. Chemical bath deposition of CdS quantum dots on vertically aligned ZnO nanorods for quantum dots-sensitized solar cells. Electrochemistry Communications 2009;11:103–6.
[206] Sudhagar P, Jung JH, Park S, Lee Y-G, Sathyamoorthy R, Kang YS, Ahn H. The performance of coupled (CdS:CdSe) quantum dot-sensitized TiO_2 nanofibrous solar cells. Electrochemistry Communications 2009;11:2220–4.
[207] Sudhagar P, Jung JH, Park S, Sathyamoorthy R, Ahn H, Kang YS. Self-assembled CdS quantum dots-sensitized TiO_2 nanospheroidal solar cells: Structural and charge transport analysis. Electrochimica Acta 2009;55:113–7.
[208] Barea EM, Shalom M, Gimenez S, Hod I, Mora-Sero I, Zaban A, Bisquert J. Design of injection and recombination in quantum dot sensitized solar cells. Journal of the American Chemical Society 2010;132:6834–9.
[209] Chen J, Wu J, Lei W, Song JL, Deng WQ, Sun XW. Co-sensitized quantum dot solar cell based on ZnO nanowire. Applied Surface Science 2010;256:7438–41.
[210] Guijarro N, Shen Q, Gimenez S, Mora-Sero I, Bisquert J, Lana-Villarreal T, Toyoda T, Gómez R. Direct correlation between ultrafast injection and photoanode performance in quantum dot sensitized solar cells. Journal of Physical Chemistry 2010;114:22352–60.
[211] Huang S, Zhang Q, Huang X, Guo X, Deng M, Li D, Luo Y, Shen Q, Toyoda T, Meng Q. Fibrous CdS/CdSe quantum dot co-sensitized solar cells based on ordered TiO_2 nanotube arrays. Nanotechnology 2010;21:375201.
[212] Li M, Liu Y, Wang H, Shen H, Zhao W, Huang H, Liang C. CdS/CdSe cosensitized oriented single-crystalline TiO_2 nanowire array for solar cell application. Journal of Applied Physics 2010;108:094304.
[213] Shen Q, Yamada A, Tamura S, Toyoda T. CdSe quantum dot-sensitized solar cell employing TiO_2 nanotube working-electrode and Cu_2S counter-electrode. Applied Physics Letters 2010;97:123107.
[214] Yang Z, Chang H-T. CdHgTe and CdTe quantum dot solar cells displaying an energy conversion efficiency exceeding 2%. Solar Energy Materials and Solar Cells 2010;94:2046–51.
[215] Chen H, Li W, Liu H, Zhu L. CdS quantum dots sensitized single- and multi-layer porous ZnO nanosheet for quantum dots-sensitized solar cells. Electrochemistry Communications 2011;13:331–4.
[216] Chen J, Lei W, Li C, Zhang Y, Cui Y, Wang B, Deng W. Flexible quantum dot sensitized solar cell by electrophoretic deposition of CdSe quantum dots on ZnO nanorods. Physical Chemistry Chemical Physics 2011;13:13182–4.
[217] Chen G, Wang L, Zou Y, Sheng X, Liu H, Pi X, Yang D. CdSe quantum dots sensitized mesoporous TiO_2 solar cells with CuSCN as solid-state electrolyte. J Nanomater 2011;2011 p. 5.
[218] Greenwald S, Rühle S, Shalom M, Yahav S, Zaban A. Unpredicted electron injection in CdS/CdSe quantum dot sensitized ZrO_2 solar cells. Physical Chemistry Chemical Physics 2011;13:19302–6.
[219] Li L, Yang X, Gao J, Tian H, Zhao J, Hagfeldt A, Sun L. Highly efficient CdS quantum dot-sensitized solar cells based on a modified polysulfide electrolyte. Journal of the American Chemical Society 2011;133:8458–60.
[220] Sun S, Gao L, Liu Y, Sun J. Assembly of CdSe nanoparticles on graphene for low-temperature fabrication of quantum dot sensitized solar cell. Applied Physics Letters 2011;98:093112.
[221] Barcelo I, Campiña JM, Lana-Villarreal T, Gómez R. A solid-state CdSe quantum dot sensitized solar cell based on a quaterthiophene as hole transporting material. Physical Chemistry Chemical Physics 2012;14: 5801–7.
[222] Jang W, Nursanto EB, Kim J, Park SJ, Min BK, Yoo K-P. Liquid carbon dioxide coating of CdS quantum-dots on mesoporous TiO_2 film for sensitized solar cell applications. Journal of Supercritical Fluids 2012;70:40–7.
[223] Jung SW, Kim J-H, Kim H, Choi C-J, Ahn K-S. ZnS overlayer on in situ chemical bath deposited CdS quantum dot-assembled TiO_2 films for quantum dot-sensitized solar cells. Current Applied Physics 2012;12: 1459–64.
[224] Lai Y, Lin Z, Zheng D, Chi L, Du R, Lin C. CdSe/CdS quantum dots co-sensitized TiO_2 nanotube array photoelectrode for highly efficient solar cells. Electrochimica Acta 2012;79:175–81.
[225] Ning Z, Yuan C, Tian H, Fu Y, Li L, Sun L, Agren H. Type-II colloidal quantum dot sensitized solar cells with a thiourea based organic redox couple. Journal of Materials Chemistry 2012;22:6032–7.
[226] Rawal SB, Sung SD, Moon S-Y, Shin Y-J, Lee WI. Optimization of CdS layer on ZnO nanorod arrays for efficient CdS/CdSe co-sensitized solar cell. Materials Letters 2012;82:240–3.
[227] Salant A, Shalom M, Tachan Z, Buhbut S, Zaban A, Banin U. Quantum rod-sensitized solar cell: nanocrystal shape effect on the photovoltaic properties. Nano Letters 2012;12:2095–100.
[228] Song X, Wang M, Shi Y, Deng J, Yang Z, Yao X. In situ hydrothermal growth of CdSe(S) nanocrystals on mesoporous TiO_2 films for quantum dot-sensitized solar cells. Electrochimica Acta 2012;81:260–7.
[229] Wang H, Luan C, Xu X, Kershaw SV, Rogach AL. In situ versus ex situ assembly of aqueous-based thioacid capped CdSe nanocrystals within mesoporous TiO_2 films for quantum dot sensitized solar cells. Journal of Physical Chemistry C 2012;116:484–9.
[230] Zhang Y, Zhu J, Yu X, Wei J, Hu L, Dai S. The optical and electrochemical properties of CdS/CdSe co-sensitized TiO_2 solar cells prepared by successive ionic layer adsorption and reaction processes. Solar Energy 2012;86:964–71.